**Title:** A GT-seq panel for walleye (*Sander vitreus*) provides a generalized workflow for efficient development and implementation of amplicon panels in non-model organisms.

**Running head**: Guide to develop and implement GT-seq panels

**Authors**: Matthew L. Bootsma[1*], Kristen M. Gruenthal[2], Garrett J. McKinney[3], Levi Simmons[1], Loren Miller[4], Greg G. Sass[5], Wesley A. Larson[6]

**Affiliations**

[1] Wisconsin Cooperative Fishery Research Unit, College of Natural Resources, University of Wisconsin-Stevens Point, 800 Reserve St., Stevens Point, WI 54481, USA, mbootsma@uwsp.edu, lsimm290@uwsp.edu

[2] Office of Applied Science, Wisconsin Department of Natural Resources, Wisconsin Cooperative Fishery Research Unit, College of Natural Resources, University of Wisconsin-Stevens Point, 800 Reserve St., Stevens Point, WI 54481, USA, kristen.gruenthal@wisconsin.gov

[3] NRC Research Associateship Program, Northwest Fisheries Science Center, National Marine Fisheries Service, National Oceanic and Atmospheric Administration, 2725 Montlake Blvd E, Seattle, WA 98112, USA, garrett.mckinney@noaa.gov

[4] Minnesota Department of Natural Resources, University of Minnesota, 135 Skok Hall, 2003 Upper Buford Circle, St. Paul, MN 55108, USA, loren.miller@state.mn.us

[5] Escanaba Lake Research Station, Office of Applied Science, Wisconsin Department of Natural Resources, 3110 Trout Lake Station Drive, Boulder Junction, WI 54512, USA, gregory.sass@wisconsin.gov

[6] U.S. Geological Survey, Wisconsin Cooperative Fishery Research Unit, College of Natural Resources, University of Wisconsin-Stevens Point, 800 Reserve St., Stevens Point, WI 54481, USA, wes.larson@uwsp.edu

***Corresponding author**

**Keywords:** Amplicon sequencing, GT-seq, microhaplotype, parentage analysis, genetic stock identification, walleye

**Abstract (250 words or less)**

Targeted amplicon sequencing methods, such as genotyping-in-thousands by sequencing (GT-seq), facilitate rapid, accurate, and cost-effective analysis of hundreds of genetic loci in thousands of individuals, but studies describing detailed workflows of GTseq panel development are rare. Here, we develop a dual-purpose GT-seq panel for walleye (*Sander vitreus*) and discuss trade-offs associated with different development and genotyping approaches. Our GT-seq panel was developed using restriction site-associated DNA data from 954 individuals sampled from 23 populations in Minnesota and Wisconsin, USA. We then conducted simulations to test the utility of loci for parentage analysis and genetic stock identification and designed 600 primer pairs to maximize joint accuracy for these analyses. We conducted three rounds of primer optimization to remove loci that overamplified and our final panel consisted of 436 loci. Optimization focused on reducing variation in amplification rate among loci and minimizing the proportion of off-target sequence, both of which are important considerations for developing large GT-seq panels. We also explored different approaches for DNA extraction, multiplexed polymerase chain reaction (PCR) amplification, and cleanup steps during the GT-seq process and discovered the following: (1) inexpensive Chelex extractions performed well for genotyping, (2) the exonuclease I and shrimp alkaline phosphatase (ExoSAP) procedure included in some current protocols did not improve results substantially and was likely unnecessary, and (3) it was possible to PCR amplify panels separately and combine them prior to adapter ligation. Well-optimized GT-seq panels are valuable resources for conservation genetics and our findings should aid in their construction in myriad taxa.

## Introduction

The development of genotyping-by-sequencing (GBS) methods has allowed collection of data from thousands of markers across a genome, enabling research that was not possible using traditional genetic approaches (Davey et al., 2011; Narum et al., 2013). For example, studies using thousands of markers genotyped with restriction site-associated DNA (RAD) sequencing have shown improved sensitivity for detecting inbreeding depression (Hoffman et al., 2014), increased resolution for determining complex phylogenies (Wagner et al., 2013), and allowed researchers to observe selection on introduced alleles (Bay et al., 2019). Many genetic analyses, however, can be conducted efficiently with genotypes from tens to hundreds of single nucleotide polymorphisms (SNPs) (Anderson & Garza, 2006), making more expensive approaches such as RAD-seq unnecessary (Meek & Larson, 2019). Two such analyses that have been widely used in conservation genetics and molecular ecology for decades, are parentage analysis and genetic stock identification (GSI).

Parentage analysis involves assigning offspring to putative parents by comparing genotypes at multiple loci, while GSI infers the natal origins of individuals by leveraging baseline allele frequency estimates from populations or reporting groups. These techniques were first conducted using allozyme markers genotyped with protein electrophoresis. Although these analyses were groundbreaking, they often lacked statistical power except in cases of highly diverged stocks or simple pedigrees. The adoption of highly variable microsatellite markers in the 1990s greatly increased statistical power, allowing these two techniques to become widely adopted (Luikart & England, 1999). Despite the advances made possible by microsatellites, problems associated with homoplasy (Garza & Freimer, 1996), locus discovery (Navajas et al.,

79 1998), and reproducibility among laboratories led researchers to explore the potential of biallelic
80 SNPs for GSI and parentage analysis (Seeb et al., 2011).

81 Although SNPs are less powerful than microsatellites on a per marker basis, SNPs are
82 more abundant in the genome, generally have low genotyping error rates, and can be genotyped
83 using SNP panels capable of efficiently screening a large number of samples (Brumfield et al.,
84 2003; Morin et al., 2004). Early SNP panels were constrained, however, in the availability of
85 molecular markers suitable for genotyping and genotyping costs associated with 5' exonuclease
86 chemistry (Seeb et al., 2011). These constraints were significantly lessened with the proliferation
87 of next-generation sequencing (NGS) technology. For example, methods such as RADseq
88 facilitate quick and affordable discovery of thousands of candidate loci, which can then be
89 selected among for specific purposes.

90 As SNP discovery has become less prohibitive, methods of selecting the most
91 informative SNPs for a given study have advanced (Storer et al., 2012). Previous research has
92 shown that information content will vary among SNPs depending on the context within which
93 they are applied and location within the genome (i.e. coding or non-coding regions). For
94 example, Ackerman et al. (2011) found that SNPs under diversifying selection provide increased
95 accuracy and precision in GSI of sockeye salmon (*Oncorhynchus nerka*) from the Copper River,
96 Alaska. In general, previous studies have shown that GSI accuracy is generally positively
97 correlated with differentiation (e.g., $F_{ST}$) and, to a lesser extent, diversity (e.g., heterozygosity)
98 (Ackerman et al., 2011; Bradbury et al., 2011; Storer et al., 2012). Studies of SNP selection
99 methods for parentage analysis, however, have found that high diversity is the most important
100 attribute to consider when creating a panel (Baetscher et al., 2018). More recently, analytical
101 techniques have shifted towards consideration of closely linked SNPs (i.e. microhaplotypes),

102 which effectively increases the diversity at a locus and has proven useful for parentage and GSI
103 tests (Baetscher et al., 2018; McKinney, Seeb, et al., 2017; Reid et al., 2019). While obtaining
104 microhaplotypes using previous 5' exonuclease methods would require independent assays for
105 each SNP at a locus and statistical phasing, NGS technology has enabled the joint genotyping of
106 multiple SNPs within single reads, making microhaplotype data easily obtainable through a
107 simple modification in analytical approach.

108 One recently developed GBS method that improves upon previous high-throughput
109 genotyping technologies, such as 5′ exonuclease chemistry, is Genotyping-in-Thousands by
110 sequencing (GT-seq). This method enables genotyping hundreds of SNPs in thousands of
111 individuals on a single NGS lane through the use of highly-multiplexed polymerase chain
112 reaction (PCR) (Campbell et al., 2015). GT-seq does not require an allele-specific probe, can
113 genotype multiple SNPs within an amplicon using a single primer pair, and is substantially less
114 expensive than 5′ exonuclease chemistry, especially in the context of genotyping thousands of
115 individuals.

116 Despite its benefits, GT-seq is not yet widely used outside of salmonids. Early
117 applications to non-model organisms, however, have shown great promise for this method's
118 versatility, including the ability to reveal dispersal and mating patterns in a complex environment
119 (Baetscher et al., 2019), provide insight to the ecological and evolutionary dynamics of
120 secondary contact (Reid et al., 2019), and understand population diversity in systems that are
121 heavily influenced by climate change (Pavinato et al., 2019). Pedigree analysis in wild
122 populations is highly dependent upon the ability to genotype large sample sizes to increase the
123 likelihood of detecting kin relationships, toward which GT-seq is ideally suited. Moreover, GT-
124 seq has proven capable of generating high-quality genotypes from low-quality DNA samples

125 (Natesh et al., 2019; Schmidt et al., 2019), making it a viable approach for monitoring
126 endangered or elusive species.

127 While GT-seq panels have been developed to maximize accuracy for GSI (McKinney et
128 al., 2019) or parentage (Baetscher et al., 2018) analyses, the potential for developing dual-
129 purpose panels is largely unexplored. Moreover, developing GT-seq panels is a relatively
130 involved task and, to this point, there are limited resources providing standardized workflows
131 and guidelines for efficient panel construction (but see Campbell et al., 2015; McKinney et al.,
132 2019). At a basic level, panel construction involves SNP discovery, SNPs selection, primer
133 design, and panel optimization (see Baetscher et al., 2018; McKinney et al., 2019; Schmidt et al.,
134 2019); however, within this general framework there are many decision points in panel
135 development related to primer selection, multiplexing approaches, laboratory protocols, and
136 analysis parameters that have yet to be addressed. We used walleye (*Sander vitreus*) from
137 Minnesota and Wisconsin, USA, as a test case to investigate various tradeoffs associated with
138 GT-seq panel development and optimization and leveraged our collective experience to provide
139 guidelines for researchers developing GT-seq panels.

140 Walleye are an apex predator and one of the most prized sportfish throughout their native
141 and introduced range. Recently, many walleye populations have declined across the Midwestern
142 United States (Embke et al., 2019; Hansen et al., 2015; Rypel et al., 2018), prompting increases
143 in stocking efforts relative to already large and long-term regional stocking programs that have
144 existed for decades. Genetic studies have been used to guide these efforts by informing
145 broodstock selection and general stocking practices. Genetic variation in walleye from this
146 region was first characterized by Fields et al. (1997), who found geographic-based patterns of
147 genetic structure, but limitations related to sample size and molecular marker choice resulted in

148 the use of contemporary watershed boundaries as genetic management units. This research was
149 later expanded upon by Hammen and Sloss (2019), who attempted to further define genetic
150 structure in the Ceded Territory of Wisconsin, approximately the northern third of the state, and
151 test whether significant genetic structure existed between distinct hydrological basins within this
152 region. Once again, constraints associated with available molecular markers used in a system
153 with not only low differentiation, but also extensive stocking precluded definition of fine-scale
154 structure. This system provides an excellent model for applying genomic techniques to
155 discriminate populations and evaluate hatchery programs using parentage analysis.

156 Like many intricacies of genomics research, GT-seq panel development is a process that
157 is at once broadly generalizable to non-model organisms and highly specific to the taxa it is
158 applied to. While the overarching steps (Fig. 1) will remain constant, there are many decision
159 points within that will require informed thought and decision. Using walleye, a species with few
160 well-established genomic resources, as a model, we examined the methods inherent to GT-seq
161 panel development in a manner that identifies critical decision points in the process and
162 illuminates the nuances associated with them. Our overarching goal was to design a dual-purpose
163 GT-seq panel optimized for parentage analysis and GSI in walleye. The creation of this panel
164 allowed us to address the following specific objectives: (1) investigate the tradeoffs between
165 choosing markers for parentage analysis versus GSI, (2) explore the most efficient way to design
166 an optimized panel, and (3) evaluate various laboratory approaches to maximizing the efficiency
167 of GT-seq genotyping. We provide an in-depth discussion of our experiences designing the panel
168 and outline important topics that should aid researchers in designing future GT-seq panels.

169 **Materials and Methods**

170 *Sample collection*

171 Tissue samples were collected from adult walleye from 23 inland lakes across Wisconsin,
172 Minnesota, and the St. Louis River (border water) (Fig. 2a, Table 1) and stored in 95% ethanol
173 until DNA extraction. We obtained samples from as many major drainages as possible across the
174 two states, with an emphasis on the Wisconsin and Chippewa River drainages in Wisconsin,
175 which were difficult to differentiate using microsatellites (Hammen & Sloss, 2019); in
176 Minnesota, sampling focused primarily on major sources of wild broodstock for stocking
177 programs. Samples were collected by the Wisconsin and Minnesota Departments of Natural
178 Resources using fyke nets or electrofishing. Sampling took place during the spring spawning
179 runs of April 2015 and 2017 and fall surveys in August and September of 2015 and 2017.
180 Stocked individuals may be tagged, or fin clipped; we inspected all sampled individuals for tags
181 or fin clips to avoid as many individuals as possible that were of stocked origin as possible.
182 *Preparation of RAD sequencing libraries*
183 Genomic DNA was extracted in a 96-well format with Qiagen DNeasy Blood and Tissue
184 Kits. Extracted DNA was quantified using a Quant-iT PicoGreen dsDNA Assay Kit (Invitrogen,
185 Waltham, MA) and normalized to 20ng/µl. DNA was then prepared for RADseq library
186 preparation following the BestRAD protocol (Ali et al., 2016). Briefly, DNA was digested in a 2
187 µl reaction with the restriction enzyme *SbfI*, and biotinylated barcode adaptors were ligated to
188 the 5' cut ends. DNA shearing was conducted using a 12.5 µl fragmentase reaction. Library
189 preparation was conducted using an NEBNext Ultra DNA Library Prep Kit for Illumina (NEB,
190 Ipswich, MA), with a 12-cycle PCR enrichment. RAD library quality was inspected on a 2%
191 agarose gel before undergoing a final AMPure XP (Beckman Coulter, Indianapolis, IN)
192 purification and quantification on a Qubit 2.0 Fluorometer (ThermoFisher Scientific, Waltham,
193 MA). Libraries were sequenced using paired-end (PE) 150 technology on a HiSeq 4000

194 (Illumina, San Diego, CA) at the Michigan State University Genomics Core Facility or
195 Novogene Corporation, Inc. (Davis, CA). Sequencing was conducted to achieve a target of over
196 one million retained reads per individual.

197 *Analysis of RAD data to discover SNPs*

198 Loci were identified and genotyped in STACKS v.2.2 (Rochette et al., 2019) without
199 using gapped alignments. Raw reads were demultiplexed and barcodes were trimmed in
200 *process_radtags* (parameter flags: -e *SbfI*, -c, -q, -filter_illumina, -r, --bestrad). RAD-tags were
201 assembled into putative RAD loci with *ustacks* using the bounded model (bound_high = 0.05, --
202 disable-gapped) and allowing for a maximum of three nucleotide mismatches (-M = 3) and four
203 stacks per locus (-max_locus_stacks = 4), as well as a minimum depth of three (-m = 3). The
204 calling of haplotypes from secondary reads was disabled (-H). A catalog of consensus loci was
205 assembled in *cstacks* using the two individuals with the highest number of retained reads from
206 each population, allowing a maximum of three mismatches between sample loci (n = 3, --
207 disable-gapped). After matching all samples against the catalog in *sstacks* (--disable-gapped),
208 data were oriented by locus with *tsv2bam*, and individual genotypes were called in *gstacks*, with
209 paired-end reads incorporated. Genotypes were exported in variant call format (vcf) using
210 *populations*, with loose filtering parameters (SNPs present at > 5% of individuals, minimum
211 minor allele frequency of > 0.005).

212 Comprehensive filtering of individuals and genotypes was conducted in vcftools v0.1.15
213 (Danecek et al., 2011) by: 1) removing individuals missing > 20% of SNP calls, 2) removing
214 SNPs that were missing in > 20% of individuals, and 3) removing SNPs that were not in the first
215 140 base pairs of the RAD-tag, effectively reducing the dataset to include SNPs detectable using
216 single-read (SR) 150 sequencing to simplify downstream amplicon design; to control for

217 genotyping error, SNPs with a minor allele count ≤ 3 were also removed. Putative duplicated loci
218 were identified in HDplot (McKinney, Waples, et al., 2017) (H > 0.5, -7 < D < 7) and removed
219 with vcftools. Retained individuals and SNPs were used to form whitelists for input into
220 *populations* that output a filtered vcf of multi-SNP haplotypes, which was then filtered to remove
221 loci with more than 10 alleles and used in simulations for locus selection. We also estimated
222 single-SNP $F_{IS}$ across all populations using diveRsity v1.9.90 (Keenan et al., 2013) and excluded
223 any SNPs with $F_{IS}$ values > 0.2 or < -0.2 from locus selection. Additionally, loci with a SNP in
224 the first 10 base pairs of the RAD-tag were excluded to allow room for forward primer design.
225 *Analysis of population structure, locus selection, and panel assessment*
226 To understand population structure in our system and ensure that selected loci could
227 facilitate accurate parentage assignment and GSI, we evaluated patterns of genetic divergence
228 using pairwise $F_{ST}$ (Table S1) estimated in Arlequin v3.5.2 (Excoffier & Lischer, 2010) and
229 constructed a dendrogram (Fig. 2b) using Nei's distance in poppr v2.8.2 (Kamvar, Tabim, &
230 Grünwald, 2014). These analyses facilitated identification of population pairs that would be
231 challenging to discriminate and supported historical data suggesting several populations were
232 founded from hatchery sources located outside of their drainage basin (Escanaba Lake, Sanford
233 Lake, and Lake Millicent in Wisconsin); these populations were removed from simulations of
234 panel accuracy to ensure that selected loci would best represent the natural genetic patterns of the
235 region.
236 After initial population genetic analyses, loci were selected for primer development by
237 constructing several test panels from the RAD data and simulating assignment accuracy for
238 parentage and GSI. Previous research suggested that choosing loci with greater genetic
239 differentiation (e.g., $F_{ST}$) should maximize accuracy for GSI (Ackerman et al., 2011; Storer et

240 al., 2012), while choosing loci with higher diversity (e.g., heterozygosity and number of alleles)
241 maximizes accuracy for parentage (Baetscher et al., 2018). We therefore constructed the test
242 panels using single-SNP $F_{ST}$ estimated in diveRsity v1.9.90 (Keenan et al., 2013) as well as
243 expected heterozygosity at a multi-SNP haplotype ($H_{E_mhap}$ ) and the number of alleles at a locus
244 estimated in adegenet v2.1.1 (Jombart & Ahmed, 2011). All simulations were conducted with
245 genotypes coded as multi-SNP haplotypes.

246 GSI accuracy for each panel was assessed via 100% simulations implemented in rubias
247 (Moran & Anderson, 2018) using the *assess_reference_loo* function (mixsize = 200, reps =
248 1000). Populations were aggregated into reporting units based on hydrological basins (Table 1).
249 Collections within a simulation were drawn from a Dirichlet distribution with all parameters
250 equal to 10 (i.e., each simulation's prior contained approximately equal proportions of each
251 population for the given reporting unit). Individuals were assigned to reporting groups if they
252 had a cumulative probability of > 70%. Unfortunately, limited sample sizes in some reporting
253 units prevented creation of separate training and holdout datasets as suggested by Anderson
254 (2010), thus assignment accuracies presented here may be upwardly biased and would need to be
255 reassessed more thoroughly for populations involved in an applied study.

256 Parentage simulations were run in CKMRsim (Anderson,
257 https://zenodo.org/record/820162), which employs a variant of the importance-sampling
258 algorithm of Anderson and Garza (2006) that allows for more accurate estimates of very small
259 false-positive rate (FPR: per-pair rate of truly unrelated individuals being inferred as related)
260 relative to those obtained using standard Monte Carlo methods (Baetscher et al., 2018).
261 Parentage analyses were conducted following the methods of Baetscher et al. (2018), whereby
262 log-likelihood ratios between a tested relationship and the hypothesis of no relationship are

263 computed from the calculated probabilities of genotype pairs for related individuals simulated
264 from allele frequency estimates. Distributions of simulated log-likelihood ratios are then used to
265 compute FPRs. Using this approach, we estimated FPRs for parent-offspring (PO), full-sibling
266 (FS), and half-sibling (HS) relationships at false-negative rates (FNR: per-pair rate of truly
267 related individuals being inferred as unrelated) ranging from 0.01 to 0.1.

268 Panels of 600 unique loci were iteratively selected, choosing loci based first on rank
269 $F_{ST}$ then rank $H_{E_mhap}$, and their utility was tested by conducting GSI tests and parentage
270 simulations. We ultimately defined three panels of 600 loci that best described the tradeoffs
271 between markers selected based on $F_{ST}$ and heterozygosity. Loci in these panels were chosen by
272 selecting 1) the top 600 loci based on $F_{ST}$, 2) the top 300 loci based on $F_{ST}$ and 300 based on
273 $H_{E_mhap}$, and 3) the top 600 loci based on $H_{E_mhap}$. These panels are hereafter referred to as
274 $F_{ST_600}$, Composite$_{_600}$, and Diversity$_{_600}$, respectively. Through further testing, we determined
275 that a variation of the Composite$_{_600}$ panel, with 250 loci based on $H_{E_mhap}$ and 350 loci based on
276 $F_{ST}$, delivered optimal performance for GSI and parentage analyses and proceeded to design
277 primers for the selected loci.

278 *Primer Design*

279 To design PCR primers for the selected loci, their consensus sequences were subset
280 from the STACKS catalog into a FASTA file for import into Geneious Prime® 2019.1.1
281 (https://www.geneious.com). The vcf file produced in the vcftools step containing all SNPs and
282 alleles within a consensus sequence was included to ensure primers were properly designed (i.e.,
283 should a SNP fall within a primer binding region, a degenerate nucleotide could be inserted or
284 the primer re-designed). Primer pairs were iteratively designed, with optimal target parameters
285 defined as a primer length of 20 bp, product size of 140 bp to facilitate genotyping with SR

286 chemistry, $T_m$ of 60° C, GC content of 50%, and no more than four of the same base repeated
287 consecutively (i.e., poly-X repeats). Primers identified as matching one or more off-target sites,
288 which could lead to amplification of multiple products, were redesigned. Given that not all 600
289 candidate loci initially identified were suitable candidates for primer development, we continued
290 to iteratively select loci and design associated primers until we reached our target of 600 loci.
291 Unfortunately, the loci selected for primer design were based on data containing a subset of
292 individuals with discordant encoded and true identities as a result of transposition of barcodes
293 during demultiplexing. Despite these discrepancies, the effect was likely minor as only 8% of
294 individuals were incorrectly assigned to reporting units prior to simulation. Simulation results
295 shown here were conducted using corrected data.

296 *GT-seq optimization*

297 GT-seq was conducted following the methods of Campbell et al. (2015), with
298 modification to the multiplex thermal cycling conditions (95 °C hold for 15 min; five cycles of
299 95 °C for 30 s, 5% ramp to 57 °C for 2 min, 72 °C 30 s; and 10 cycles of 95 °C for 30 s, 65 °C
300 for 30 s, and 72 °C 30 s) and post-normalization dual-sided SPRI size-selection and purification
301 (0.6X plus 0.4X) to further restrict the product size range (e.g., primarily toward removal of
302 primer inter-hybridization). Final library quality control consisted of confirmation of
303 amplification and barcoding by SYBR Green-based RT-qPCR (Stratagene Mx3005P QPCR
304 System, Agilent, Santa Clara, CA), visualization on a 2% agarose E-Gel (Invitrogen, Carlsbad,
305 CA), and quantification using picogreen. Libraries were then sequenced at the University of
306 Wisconsin-Madison Biotechnology Center (UWBC) DNA Sequencing Facility on a MiSeq
307 (Illumina) using 2 × 150 bp flowcells.

308 Demultiplexed amplicon sequencing data were processed using *GTscore v1.3*
309 (McKinney et al., 2019). *GTscore* generates *in-silico* primer-probe sequences from a catalog of
310 loci generated in STACKS, that are then matched to amplicon sequences and call genotypes for
311 individual SNPs as well as multi-SNP haplotypes. *GTscore* also enables separation of on-target
312 sequence reads (i.e., reads containing both an *in-silico* primer and associated probe) from reads
313 produced as a result of primer cross-hybridization. Primer-probe file development was
314 accomplished with *sumstatsIUBconvert.pl* by obtaining the IUB code information for each SNP
315 from the sumstats.tsv file produced in the STACKS pipeline, converting catalog sequences
316 produced in the STACKS pipeline to FASTA sequences using *catalog2fasta.pl*, and merging
317 IUB code information with the catalog.fasta using *fasta2IUB.pl*. This primer-probe file was then
318 input for *AmpliconReadCounter.pl*, along with an individual's fastq file, to produce read count
319 summaries of primers and probes.
320 Overall, we conducted three rounds of panel optimization to identify and remove loci
321 that had disproportionately high amplification rates (i.e., "overamplifiers") and ensure that our
322 panel was capable of delivering a high proportion of on-target reads for each locus as well as
323 homogeneous amplification rates among loci. The first round of optimization used DNA from a
324 single walleye from Sanford Lake, WI, while the second and third rounds were conducted on
325 subsets of 24 individuals from each of four populations (96 individuals total) originally included
326 in the RADseq study: Delavan Lake, Medicine Lake, and the Wolf River in Wisconsin and the
327 Pine River in Minnesota. Upon completing the final optimization, the characteristics of retained
328 loci were compared to those of loci culled from the panel. This was done by performing a
329 Welch's two sample t-test ($\alpha = 0.05$) between the GC:AC ratio of primers that were retained and

330 those culled and between the GC:AC ratio of DNA templates retained and culled, based on the
331 first 140 bp of the template as this was the region in which SNPs were targeted.
332 GT-seq libraries from each round were collectively analyzed for PCR accuracy
333 and uniformity. Accuracy was measured by calculating the proportion of reads containing *in-*
334 *silico* primer sequences (total reads) relative to those that also contained *in-silico* probes.
335 Uniformity of amplification among loci was determined by calculating the proportion of total
336 reads that were allocated to the top 10% of loci, based on locus read counts (prop_reads_T10); if
337 amplification was perfectly uniform across loci, we would expect prop_reads_T10 to account for
338 exactly 10% of total reads. Given that amplification rates vary substantially within a panel, we
339 compared among locus performance by plotting the relative $\log_{10}$ abundance of total and on-
340 target reads at each locus in descending order, which facilitated visual identification of
341 overamplifiers. As among-locus amplification rates evened out after the first optimization, the
342 on-target proportion of reads at each locus became a factor in retaining or excluding loci during
343 the second optimization.
344 *Testing methodological modifications and performance analysis*
345 During panel optimization, we compared the quality of GT-seq libraries prepared
346 from DNA extracted with Qiagen DNeasy and a more cost-effective chelating resin-based
347 procedure. Performance of libraries was compared using Bonferroni corrected ($\alpha = 0.016$)
348 Tukey's HSD for the number of on-target reads and the proportion of total reads that were on-
349 target, after determining whether significant differences existed among libraries via a one-way
350 ANOVA ($\alpha = 0.05$). DNA was extracted from the 96 test individuals twice, first using Qiagen
351 DNeasy and again with a 10% Chelex 100 (200-400 mesh; Bio-Rad, Hercules, CA) solution
352 containing 1% each of Nonidet P-40 and Tween 20 (Millipore Sigma, St. Louis, MO).

353 Additionally, we aimed to further reduce the cost per sample by evaluating the need for certain
354 library preparation steps. Specifically, we compared results with and without the exonuclease I
355 and shrimp alkaline phosphatase (ExoSAP) procedure included in Campbell et al. (2015) to
356 remove PCR inhibitors and free nucleotides. GT-seq was therefore conducted on all individuals
357 in triplicate: 1) Qiagen with ExoSAP, 2) Chelex with ExoSAP, and 3) Chelex without ExoSAP,
358 and all tests were sequenced on the same MiSeq lane. Finally, we tested whether the number of
359 loci that could be genotyped simultaneously could be increased by conducting multiple PCRs.
360 We accomplished this by dividing our optimized primer panel into two non-overlapping primer
361 pools before multiplex PCR amplification. We then merged PCR products from the separate
362 pools prior to the barcoding PCR. The sequencing performance of this joint panel was then
363 compared to the single multiplex containing the full panel using a Welch's two sample t-test ($\alpha =$
364 $0.05$).

365 We examined genotype concordance between RADseq and GT-seq across GT-seq
366 read depths using the fully optimized panel in the third round. Genotypes were called using
367 *PolyGen* (McKinney et al., 2018), an extension of the *GTscore* pipeline that uses the same
368 maximum-likelihood algorithm as STACKS v1 for diploid, bi-allelic loci. Because low read
369 depths can lead to high estimates of genotyping error, thereby increasing rates of allelic dropout
370 (Catchen et al., 2013), genotypes were only compared if they had greater than 60× coverage in
371 RADseq. We then modeled the relationship between GT-seq read depth and genotype
372 concordance using only read depths with more than 30 genotypes to ensure that estimates of
373 genotype concordance at a given depth had adequate sample sizes.

374 As a final proof of concept, we tested the optimized panel on a sample of 570 walleye
375 obtained from Escanaba Lake, WI, using the methods described above to estimate the variance in

376 read depth among loci within a pool. We retained only loci present in more than 70% of
377 individuals and individuals genotyped at more than 70% of loci.

378 **Results**

379 *Analysis of ascertainment dataset*

380 A total of 954 individuals from 23 populations were RAD sequenced, with an average of
381 42 individuals per population (Table 1). Sequencing yielded 1,313,358 retained reads on average
382 per individual (range = 8,941 - 8,176,163). Initial sequence data were used to identify 682,223
383 putative SNPs. After passing sequence data through quality filters, 839 individuals and 20,597
384 SNPs were retained (Table S2).

385 Population estimates of $H_O$ (0.144 - 0.179), allelic richness (1.498 - 1.674), and $F_{IS}$ (-
386 0.050 - 0.017) were relatively similar across locations (Table 1). Populations from Minnesota
387 had slightly lower diversity, which may be due to ascertainment bias as 14 of the 23 populations
388 were from Wisconsin. The highest genetic differentiation was observed between populations
389 from Minnesota and Wisconsin, with further structuring by drainage basin within each state (Fig.
390 2b, Table S1). Structuring was higher in Minnesota, with most populations showing a relatively
391 high degree of isolation (average $F_{ST}$ = 0.07, Table 2). Structure in Wisconsin was shallower
392 (average $F_{ST}$ = 0.03, Table 2) and only loosely correlated with drainage basins. From these
393 results, we constructed 13 reporting groups to facilitate GSI to identifiable genetic units (Table
394 1). All the reporting groups from Minnesota contained single populations, whereas in Wisconsin,
395 while the Rock-Fox and Wolf River groups contained single populations, the Wisconsin and
396 Chippewa River groups each contained five populations. Some single populations in the
397 Wisconsin and Chippewa Rivers were distinctly identifiable (e.g., Eau Claire River, Medicine

398 Lake), but we grouped these populations within their drainage basin of origin as the panel will
399 likely be used this way for management purposes.

400 *Locus selection and panel assessment*

401 GSI accuracy was similar among the three panels, with < 1% difference in average
402 accuracy between the panel with loci chosen based solely on differentiation ($F_{ST}$_600) and the
403 panel based solely on diversity (Diversity_600) (Fig. 3, Table 3). Average assignment accuracy
404 was > 90% for nine of the 13 reporting units in all panels (Fig. 3a). The remaining four reporting
405 units had average assignment accuracies ranging from 78% to 86%. Three of these units (upper
406 Chippewa River, WI; St. Louis River, MN/WI; and Red Lake, MN) are known to have admixed
407 stocking histories, while the fourth, North Fork Crow River, MN, included Lake Koronis, which
408 had the fewest individuals retained after filtering (n = 15). Misassigned individuals from the St.
409 Louis River, MN, and Red Lake, MN groups primarily assigned to the Pike River, MN, an
410 unsurprising result given that fish from the Pike River contributed to the recovery of the
411 collapsed walleye fishery in Red Lake (Logsdon et al., 2016) and fish in the St. Louis River
412 watershed. Misassignments from the Upper Chippewa basin primarily assigned to the Upper
413 Wisconsin basin due to the lower differentiation described previously.

414 The populations with the lowest assignment accuracies were found in the Chippewa
415 River and Wisconsin River reporting groups (Table S3, S4, S5), particularly in northern
416 Wisconsin near the headwaters of the Chippewa and Wisconsin River drainages, and included
417 Big Arbor Vitae Lake ($F_{ST_600}$ accuracy = 74%), Manitowish Lake ($F_{ST_600}$ accuracy = 58%), and
418 Turtle Flambeau Flowage ($F_{ST_600}$ accuracy = 63%). A large portion (> 10%) of the simulated
419 individuals from these populations could not be assigned to any population, providing further
420 support for the genetic similarity of these two reporting groups. A high proportion of individuals

421 from Big Arbor Vitae Lake were assigned to Manitowish Lake (12%) and vice versa, from
422 Manitowish Lake to Big Arbor Vitae Lake (20%). Most misassignments in the Turtle Flambeau
423 Flowage were to Kawaguesaga Lake (16%). Populations with high misassignment rates also
424 tended to have short branch lengths in the dendrogram and were often located near the root of a
425 clade (Fig. 2b). Furthermore, the two populations from the upper Chippewa basin (Manitowish
426 Lake and Turtle Flambeau Flowage) had lower pairwise $F_{ST}$ values, on average, relative to
427 populations from the upper Wisconsin basin than they did with other populations from the upper
428 Chippewa basin.

429 The Diversity$_{_600}$ panel had the highest accuracy for assigning kin relationships, the
430 Composite$_{_600}$ panel showed intermediate performance and the $F_{ST_600}$ panel had the lowest
431 accuracy rate (Fig. 3b, Table 3). For all panels, FPRs were $< 10^{-20}$ for PO and FS relationships,
432 indicating all panels would perform adequately for reconstructing most relationships in most
433 study systems. Inter-panel performance did, however, range widely, from an FPR of $4.68 \times 10^{-34}$
434 for $F_{ST}$_600 to $2.74 \times 10^{-80}$ for Diversity$_{_600}$ panel at an FNR of 0.01. Within panels, FPR was
435 inversely related to FNR.

436 Primers were designed using a modified Composite_600 panel, with 250 loci chosen
437 based on $H_{E_mhap}$ and 350 chosen based on $F_{ST}$, as this panel delivered the best joint accuracy for
438 GSI and kinship analyses (Fig. 3, Table 3). Of the initial 600 loci initially selected for primer
439 design, 100 were not suitable for primer design, and thus, iterative selection of loci meeting
440 primer design requirements was continued until the targeted number of $F_{ST}$ and diversity markers
441 was met.

442 *GT-seq optimization*

443 Initial amplification and MiSeq sequencing of all 600 loci yielded 4,655,071 reads
444 containing intact i7 barcode sequences, with 4,150,910 reads (89%) matching *in-silico* primer
445 sequences. Locus specificity was considered via the proportion of total reads that were on-target,
446 which was 1,031,707 (24.9%) (Table 4). In terms of amplification uniformity among loci,
447 prop_reads_T10 accounted for 3,526,201 (85.0%) of the 4,150,910 total reads. A cutoff of 3,000
448 reads per locus was then visually identified (Fig. 4a); loci producing more than 3,000 reads (n =
449 123) were deemed overamplifiers and discarded prior to further optimization.
450 For the second round of optimization, the remaining 477 primers pairs produced
451 12,653,262 reads containing intact i7 barcode sequences, and 9,347,591 (74%) matched *in-silico*
452 primer sequences. Locus specificity improved, with 3,268,293 (35.0%) of the total reads
453 successfully aligning to *in-silico* probe sequences (Table 4). Improvement was also observed in
454 the uniformity of amplification across loci, with prop_reads_T10 equating to 72.5% (6,776,302)
455 of total reads. Because locus performance was less variable in this round of testing, the
456 individual on-target proportion of reads at a locus was also considered while culling undesirable
457 loci. As such, loci visually identified as overamplifiers were again discarded if they did not
458 display high on-target read proportions (n = 41, Fig. 4b).
459 The third GT-seq test was used to determine the functional performance of the panel and
460 aimed to target 858 SNPs across 436 loci (Fig. 4c). This test produced 7,282,101 reads with
461 intact i7 barcodes, and 6,827,424 (94%) matched to *in-silico* primers. Locus specificity of primer
462 pairs improved greatly in this test, as 6,262,523 (91.7%) of the total reads were also on-target
463 (Table 4). Likewise, the variation in amplification rates across loci decreased as evidenced by
464 prop_reads_T10 decreasing to 36.6% (2,148,932) of the total reads.

465 Upon completion of panel optimization, a small but significant difference was observed
466 between the GC content of primers that were retained (mean = 49.2%) and primers that were
467 removed (mean = 51.4%, df = 602, t = 5.4, $p < 0.001$). Similar differences were found when
468 comparing the GC content of the DNA template; significantly higher GC proportions were
469 present in templates that were culled from the panel (mean = 47.8%) than templates that were
470 retained (mean = 45.5%, df = 359, t = 3.8, $p < 0.001$). Additionally, a total of 88 primer pairs in
471 the original panel contained at least one degenerate nucleotide, 72 (81%) of which were in the
472 forward primer. After optimization, 56 of the initial 88 (64%) were retained. In comparison, of
473 the 512 initial primer pairs that did not have degenerate primers, 380 (74%) were retained. The
474 average $F_{ST}$ for the most informative SNP at a locus and the average $H_{E_mhap}$ did not change
475 appreciably between the initial and fully optimized panels (Table 4).

476 *Methodological modifications and performance analysis*

477 Significant differences for on-target read counts and the proportion of total reads that
478 were on-target were detected among genomic DNA extraction and purification method
479 combinations. Subsequent analysis using Tukey's HSD revealed that Chelex-extracted DNAs
480 produced the highest on-target read count, and Qiagen-extracted DNAs with ExoSAP-
481 purification produced the lowest (Fig. 5, $p < 0.001$). While the proportion of on-target reads did
482 not differ between Chelex with ExoSAP and Qiagen with ExoSAP, both methods produced a
483 significantly lower proportion of on-target reads than the Chelex-only library (Fig. 5, $p < 0.001$).
484 Additionally, when comparing results from the full panel of 436 primer pairs to those obtained
485 using the same panel divided into two unique multiplexes of 209 and 227 primer pairs (n = 436)
486 and repooled prior to barcoding, no significant differences were found in total primer reads (df =

860, t = 0.10, p = 0.92), on-target reads (df = 858, t = 0.16, p = 0.87), or the proportion of total reads that were on target (df = 806, t = 0.66, p = 0.51).

A total of 4,063 genotypes across 406 loci (820 SNPs) could be used in comparisons between GT-seq data and those obtained from the original RAD study. Of these genotypes, 96.6% of calls were identical between methods, and modeled expectations of genotype concordance (residual sum of squares = 0.02) indicated that a concordance rate of 99.0% could be expected at a GT-seq read depth of 31 (Fig. 6).

For a final proof of concept, a new sample of 570 walleye was sequenced using the current panel of 436 loci. After filtering, 551 individuals and 303 loci were retained with an average of 32.9 (SD = 29.1) reads per locus; 116 of the 303 loci exhibited an average coverage greater than the 31× target identified for 99.0% genotyping concordance (Fig. 7). The average percent of missing data was 6.4% (SD = 13.0%) across individuals and 30.0% (SD = 38.0%) across loci.

**Discussion**

GT-seq and other amplicon sequencing methods have tremendous potential for facilitating high-throughput genotyping in non-model organisms (Meek & Larson, 2019). The general steps for GT-seq panel development: SNP ascertainment, SNP selection, primer design, and panel optimization have been previously detailed (Baetscher et al., 2018; McKinney et al., 2019; Schmidt et al., 2019); however, the process of GT-seq panel development is not static. Here, we leverage our experiences developing a GT-seq panel for walleye with testing various aspects of the GT-seq methodological process to provide additional guidelines usable by other researchers to simplify panel construction and validation, particularly in non-model species. Our walleye panel has the necessary power to conduct GSI in a study system with highly variable

510 degrees of genetic differentiation and perturbation by historical stocking, while also being
511 capable of identifying PO and FS relationships within large populations. The robust performance
512 of our panel was facilitated by exploring the upper limits of how many loci a GT-seq panel can
513 target and the trade-offs between choosing loci for GSI versus parentage analysis. The
514 information presented here will aid in the efficient creation of multipurpose GT-seq panels in
515 organisms with little to no available genomic resources.

516 *Patterns of population structure: historical stocking influences GSI accuracy*

517 The largest genetic differentiation in our data was observed between populations from
518 Wisconsin and Minnesota; this structure was likely the result of recolonization from different
519 refugia following the Wisconsin glaciation, which ended ~10,000 years ago. A range-wide
520 analysis of walleye genetic structure using microsatellite loci produced similar patterns, with the
521 most genetically independent populations found in northern Minnesota and Canada (Stepien et
522 al., 2009). Additionally, we found that while populations in Minnesota displayed strong isolation
523 on relatively small spatial scales, broad-scale patterns of isolation were less evident in
524 Wisconsin. In particular, the Ceded Territory of Wisconsin, which included our Chippewa River
525 and Wisconsin River reporting groups, displayed patchy and low genetic structure overall. It is
526 likely that structure in this region has been compromised by stocking. Hammen and Sloss (2019),
527 for instance, observed that several populations of walleye in the upper Chippewa were more
528 genetically similar to populations in the upper Wisconsin than to other populations in the upper
529 Chippewa, while nongame species in the Ceded Territory of Wisconsin displayed patterns of
530 genetic divergence strictly associated with drainage basin boundaries (Westbrook, 2012). We
531 also observed that four proximate populations spanning the Chippewa and Wisconsin River
532 boundaries were nearly indistinguishable (Turtle Flambeau Flowage, Manitowish Lake,

533 Kawaguesaga Lake, Big Arbor Vitae Lake). These populations are within 50 km of each other
534 and are located near a state walleye hatchery in Woodruff, Wisconsin, that has historically used
535 broodstock solely from the Wisconsin River drainage basin. It is therefore highly likely that the
536 genetic similarity of these four populations is due to stocking. Several of the sampled
537 populations from Minnesota also had poorly documented stocking histories yet they remained
538 highly distinct. Genetic structure in Minnesota may have been less eroded if local, genetically
539 similar sources were used, stocking was into larger, healthier resident populations, or stocking
540 was less intense or ended a longer time ago.

541 Despite the challenges posed by low $F_{ST}$ and evidence of supplemental stocking altering
542 genetic structure in some populations, the SNPs discovered here provide greatly increased
543 resolution for defining reporting units across the Midwestern, USA. Additionally, simulations
544 suggested that a panel of several hundred loci would be highly capable of conducting individual-
545 based GSI for most genetic units in the region. Given the regional complexity, however,
546 improvements to accuracy could be made by further sampling areas that have shown
547 heterogeneous signals of genetic structure (e.g., due to stocking). For example, increased
548 sampling effort directed at the Chippewa and Wisconsin Rivers' drainage basins could prove
549 especially beneficial as analyzing populations in the lower reaches of each basin may provide a
550 better understanding of signals of historical recolonization, while populations in the upper
551 reaches (e.g., Ceded Territory of Wisconsin) could better define the effects stocking may have
552 had. Additional samples could also serve as a holdout dataset, as suggested by Anderson (2010),
553 to test the assignment accuracy of our panel.

554 *Tradeoffs associated with choosing loci based on differentiation versus diversity*

555 We evaluated the tradeoffs associated with selecting SNPs based on differentiation or
556 diversity and found that there was relatively little variation in GSI accuracies across panels.
557 Markers selected based on differentiation have been shown to provide increased resolution for
558 defining reporting groups in systems with low levels of genetic structure (Larson et al., 2014;
559 McKinney et al., 2019). This approach has not, however, been applied to systems where stocking
560 may be a major factor for reduced levels of population structure, such as in upper Midwestern,
561 USA, walleye. Interestingly, we found that assignment accuracies with our smaller panels was
562 relatively similar to accuracies obtained using ~30,000 SNPs discovered with RAD-seq (data not
563 shown). This suggests that assignment accuracy in our system may be limited more by biological
564 realities associated with human-mediated gene flow than by the power of our genetic markers.
565 Further increases in assignment accuracy are therefore likely to be realized through sampling of
566 additional populations and a more refined understanding of population history as opposed to
567 genotyping additional markers.
568 Conversely, we found that FPRs for assigning kin relationships were highly variable
569 among panels, with the microhaplotype diversity-based panel displaying the lowest FPRs by
570 several orders of magnitude for each kin relationship (Table 3). This contrast in inter-panel
571 variation between GSI and kinship simulations is reflective of the variation in information
572 content of each panel (Fig. S1), and supports previous findings that while microhaplotype
573 information provided added benefit to both applications, the greatest increase in assignment
574 accuracy will likely be for kinship analysis (Baetscher et al., 2018; McKinney, Seeb, et al.,
575 2017). When attempting to target microhaplotype loci via GT-seq, attention should be given to
576 the number of SNPs one aims to genotype within a locus, as attempting to include loci with too
577 many SNPs may result in targeting repetitive regions that fail to amplify properly in a multiplex.

578 The expected maximum number of alleles per locus and the degree to which loci with large
579 numbers of alleles perturbs primer design will likely vary among taxa. We chose a cutoff of 10
580 alleles per locus as this appeared to be a natural break point in the allele distribution for walleye;
581 we suggest that researchers investigate this in their system and come up with a logical cutoff
582 prior to selecting loci. Finally, while our results suggested this panel could facilitate HS
583 identification in small systems, performing this task in large systems would likely require more
584 loci. Our tests of panel implementation suggest this could be achievable by combining PCR
585 products from several panels within individuals prior to barcoding.

586 *Optimizing primer design and removing overamplifying loci*

587 The main objective of GT-seq primer development is to produce a single pool of primer
588 pairs that will amplify uniformly, while retaining as many loci as possible. To achieve this, it is
589 important to minimize heterogeneity of primer and product characteristics (e.g., primer size,
590 product size) and to understand that the highly multiplexed PCR required by GT-seq can be
591 complicated by hairpin- and inter-primer hybridization artifacts. To best control PCR artifacts, it
592 is important to avoid developing primers with complimentary regions (e.g., complimentary 3'
593 regions and self-complementarity) and apply conservative thresholds to the upper $T_m$ of primer
594 design parameters (Rychlik, 1993). Incorporating loci with multiple SNPs can lead to further
595 difficulties when the ideal priming region also contains a SNP. We found that, while degenerate
596 primers could be successfully amplified in a multiplex, they were culled during optimization at a
597 higher rate than non-degenerate primers. Further performance benefits could be gained from
598 examining DNA template quality beyond just the availability of priming regions, as shown by
599 Benita et al. (2003) who found regionalized GC content of template DNA to be a predictor of
600 PCR success. This was supported by our data, as loci removed from the panel during

601 optimization displayed significantly higher GC content in the amplicon and primer. Finally,
602 while GT-seq primers can theoretically be designed for a range of amplicon sizes, we suggest
603 that researchers design panels targeting similarly sized products that can be sequenced using
604 PE150 technology. Panels containing similarly sized and relatively short amplicons should
605 reduce variation in amplification rates (Baetscher et al., 2018) and ensure that genotyping is
606 robust to variation in sample quality. Moreover, PE150 sequencing is common to benchtop and
607 core facility sequencing platforms, such as Illumina® MiSeq and HiSeq.

608 In exploring the upper limits of how many loci a GT-seq panel can target, we found that
609 the number of amplicons reliably genotyped in a single pool is highly dependent on variable
610 rates of amplification among primer pairs during PCR and, to a lesser extent, the degree of
611 primer specificity. Despite efforts to limit primer inter-hybridization through diligent primer
612 design, the presence of overamplifying loci is likely inevitable during early phases of panel
613 development (see also McKinney et al. 2019). We found it best to focus primarily on the
614 uniformity of amplification within the primer pool in early optimization steps, by removing
615 primer pairs found to overamplify. Although achieving perfect uniformity is challenging,
616 application of strict cutoffs during initial optimization steps likely results in a final panel that is
617 less influenced by overamplification, thereby increasing the upper limit of GT-seq performance.
618 The importance of this was illustrated by prop_reads_T10 reducing from 85.0% of all primer
619 reads to 36.6% after optimization. Likewise, on-target rates were greatly improved by addressing
620 overamplification, as demonstrated by the on-target proportion of reads increasing from 24.9% to
621 91.7% by the third test.

622 *Further optimization of the GT-seq protocol*

623 Although there may be an upper as-yet-unidentified limit in the number of primers that
624 can be included in a single primer pool, we found that the total number of loci targeted can be
625 increased by PCR amplifying multiple primer pools separately on a sample and pooling PCR
626 products within individuals prior to barcoding. This approach could be used to genotype multiple
627 complementary or even independent GT-seq panels using the same primer tail systems at a small
628 cost increase compared to genotyping a single panel, as the most expensive steps in the GT-seq
629 protocol (e.g., DNA normalization) are only conducted once (Campbell et al., 2015). Combining
630 multiple panels could facilitate genotyping of > 1,000 loci rather than a few hundred, providing
631 greatly increased power for kinship analysis and GSI (Baetscher et al., 2018; McKinney, Seeb, et
632 al., 2017). Additionally, further optimization of individual panels could be conducted by
633 manipulating the initial concentrations of primer pairs based on observed panel performance,
634 reducing the concentration of loci that appear to overamplify. While this process would be
635 cumbersome to perform by hand, a liquid handling robot could enable a researcher to fine-tune
636 the performance of existing and new panels alike, thereby enhancing efficiency.
637 DNA extraction can comprise a large portion of the total cost of genetic analysis,
638 especially for relatively affordable approaches such as GT-seq, in terms of finances and time.
639 Extractions using chelating beads provided a cost-effective alternative to more expensive salting-
640 out approaches, such as Qiagen DNeasy kits. Chelating extractions, however, can also produce
641 lower quality DNA and may include suspended impurities (Singh et al., 2018). Campbell et al.
642 (2015) did show that GT-seq can be conducted using DNA from chelating extractions but did not
643 directly compare results using multiple extraction protocols. Here, we directly showed that cost-
644 effective chelating extractions can produce equally high quality, if not superior, sequence data
645 compared to more expensive methods. Although consideration should be given to the quality of

646 tissue samples, the chelating approach appears to be a viable approach for reducing per-sample
647 costs with GT-seq. It is important to be aware that proper laboratory technique is essential when
648 using this method, however, as chelating beads will inhibit PCR and greatly reduce library
649 product yields. This may be especially problematic when using a liquid handling robot that is
650 unable to visually detect chelating beads. Therefore, we suggest researchers carefully pipette the
651 DNA-containing supernatant from chelating resin extractions by hand into a secondary container
652 (e.g., 96-well PCR plate) before aliquoting DNA with a robot. Finally, we found that the
653 ExoSAP procedure included in the original GT-seq protocol did not produce higher quality data
654 and was not necessary for our purposes; removing this step from the protocol will further reduce
655 GT-seq costs and time commitment.

656 *Suggestions for designing GT-seq studies and conclusions*

657 A major consideration when designing a GT-seq panel is deciding how large of an
658 ascertainment dataset is necessary. We constructed a comprehensive ascertainment set with
659 RAD-seq, which was expensive and resource intensive. Despite this, we found that the panel
660 chosen based on diversity produced similar results to the panel chosen based on differentiation.
661 In our case, we believe that a smaller ascertainment set of ~96 individuals sampled from across
662 the same geographic range may have resulted in a panel of relatively similar quality. Smaller
663 ascertainment datasets are likely sufficient when the main applications of a given GT-seq panel
664 are kinship analysis and GSI of highly diverged populations; however, when designing GT-seq
665 panels to differentiate closely related populations (e.g. Chinook salmon *Oncorhynchus*
666 *tshawytscha* in western Alaska), accurate characterization of ascertainment populations is vital
667 (Larson et al., 2014; McKinney et al., 2019).

668 Another major consideration when conducting GT-seq analysis is deciding how deep to
669 sequence individuals. We found that a read depth of 31× could be expected to produce genotypes
670 that were 99% concordant with those derived from RADseq. Read depths were, however, highly
671 variable across loci; we only retained 303 of the 436 loci in our panel when we genotyped 536
672 individuals at an average depth of 33×. We also found that a large and variable proportion of
673 reads can be discarded prior to genotyping. Therefore, we suggest that researchers target an
674 average depth of at least 100× to ensure that most loci in the panel can be genotyped and that all
675 acquired genotypes are highly reliable. At this level of coverage, researchers could genotype
676 ~500 individuals with a panel of 500 loci on a single MiSeq lane (~25 million reads) and ~8,000
677 individuals on a HiSeq lane (~400 million reads). It is possible this level of coverage is not
678 necessary for some applications, such as GSI, but we strongly suggest obtaining high coverage
679 for more sensitive applications that require high genotyping accuracy, such as kinship analysis.
680 Finally, researchers conducting GT-seq must consider trade-offs associated with different
681 genotyping approaches. The two main approaches we are aware of are: (1) in-silico probe-based
682 methods that use pattern matching to genotype specific alleles (Campbell et al., 2015; McKinney
683 et al., 2019) and (2) alignment-based methods that call all polymorphisms in a given amplicon
684 (Baetscher et al., 2019). A major advantage of probe-based methods is that databases of probes
685 can be shared among laboratories, facilitating standardization. It is difficult, however, to discover
686 new variation with these methods, whereas alignment-based methods discover new variation by
687 default. We suggest a hybrid approach, where researchers periodically use alignment-based
688 approaches to discover new variation and add this variation to a probe database that forms the
689 basis of genotyping and standardizing genotyping among laboratories.

690 GT-seq is a powerful addition to the molecular ecologist's toolkit that facilitates rapid,
691 accurate, and cost-effective genetic analysis. Yet, creating a GT-seq panel is non-trivial, and
692 there are many considerations for maximizing the utility of this approach. We found that the
693 greatest challenge when designing our GT-seq panel was locus-specific overamplification, and
694 we suggest that researchers remove these loci liberally. We also found that chelating extractions
695 without an ExoSAP step produce high-quality results, providing a lower-cost alternative to
696 salting-out extractions. Additionally, we showed that combining multiplex PCR products from
697 multiple panels prior to barcoding can ensure additional, potentially important, loci can be
698 genotyped with only a moderate cost increase. Finally, we found that a relatively substantial
699 proportion of sequencing reads are lost before genotyping, and we suggest researchers target
700 higher sequencing coverage (100×) than may apparently be necessary to ensure that GT-seq
701 datasets are robust across loci. The GT-seq approach promises to be a mainstay of population
702 genetics for the foreseeable future, and the guidelines and suggestions outlined here may help
703 increase the effective use of this powerful method.

704 **Acknowledgements**

705 We thank field crews from the Wisconsin and Minnesota Departments of Natural Resources for
706 collecting tissue samples. We also thank Keith Turnquist from UW-Stevens Point for assistance
707 with laboratory analysis and Ana Ramón-Laca for advice regarding primer development. This
708 study was funded by the United States Fish and Wildlife Service, Federal Aid in Sportfish
709 Restoration program and the Wisconsin Department of Natural Resources. Any use of trade,
710 firm, or product names is for descriptive purposes only and does not imply endorsement by the
711 U.S. Government.

712 **References**

Ackerman, M. W., Habicht, C., & Seeb, L. W. (2011). Single-Nucleotide Polymorphisms (SNPs) under Diversifying Selection Provide Increased Accuracy and Precision in Mixed-Stock Analyses of Sockeye Salmon from the Copper River, Alaska. *Transactions of the American Fisheries Society, 140*(3), 865-881. doi:10.1080/00028487.2011.588137

Ali, O. A., O'Rourke, S. M., Amish, S. J., Meek, M. H., Luikart, G., Jeffres, C., & Miller, M. R. (2016). RAD Capture (Rapture): Flexible and Efficient Sequence-Based Genotyping. *Genetics, 202*(2), 389-400. doi:10.1534/genetics.115.183665

Anderson, E. C. (2010). Assessing the power of informative subsets of loci for population assignment: standard methods are upwardly biased. *Molecular Ecology Resources, 10*(4), 701-710. doi:10.1111/j.1755-0998.2010.02846.x

Anderson, E. C., & Garza, J. C. (2006). The power of single-nucleotide polymorphisms for large-scale parentage inference. *Genetics, 172*(4), 2567-2582. doi:10.1534/genetics.105.048074

Baetscher, D. S., Anderson, E. C., Gilbert-Horvath, E. A., Malone, D. P., Saarman, E. T., Carr, M. H., & Garza, J. C. (2019). Dispersal of a nearshore marine fish connects marine reserves and adjacent fished areas along an open coast. *Molecular Ecology, 28*(7), 1611-1623. doi:10.1111/mec.15044

Baetscher, D. S., Clemento, A. J., Ng, T. C., Anderson, E. C., & Garza, J. C. (2018). Microhaplotypes provide increased power from short-read DNA sequences for relationship inference. *Mol Ecol Resour, 18*(2), 296-305. doi:10.1111/1755-0998.12737

Bay, R. A., Taylor, E. B., & Schluter, D. (2019). Parallel introgression and selection on introduced alleles in a native species. *Molecular Ecology, 28*(11), 2802-2813. doi:10.1111/mec.15097

Benita, Y., Oosting, R. S., Lok, M. C., Wise, M. J., & Humphery-Smith, I. (2003). Regionalized GC content of template DNA as a predictor of PCR success. *Nucleic Acids Research, 31*(16), e99-e99. doi:10.1093/nar/gng101

Bradbury, I. R., Hubert, S., Higgins, B., Sharen, B., Paterson, I. G., Snelgrove, P. V. R., . . . Bentzen, P. (2011). Evaluating SNP ascertainment bias and its impact on population assignment in Atlantic cod, Gadus morhua. *Molecular Ecology Resources, 11*(s1), 218-225. doi:10.1111/j.1755-0998.2010.02949.x

Brumfield, R. T., Beerli, P., Nickerson, D. A., & Edwards, S. V. (2003). The utility of single nucleotide polymorphisms in inferences of population history. *Trends in Ecology & Evolution, 18*(5), 249-256. doi:https://doi.org/10.1016/S0169-5347(03)00018-1

Campbell, N. R., Harmon, S. A., & Narum, S. R. (2015). Genotyping-in-Thousands by sequencing (GT-seq): A cost effective SNP genotyping method based on custom amplicon sequencing. *Molecular Ecology Resources, 15*(4), 855-867. doi:10.1111/1755-0998.12357

Catchen, J., Hohenlohe, P. A., Bassham, S., Amores, A., & Cresko, W. A. (2013). Stacks: an analysis tool set for population genomics. *Molecular Ecology, 22*(11), 3124-3140. doi:10.1111/mec.12354

Danecek, P., Auton, A., Abecasis, G., Albers, C. A., Banks, E., DePristo, M. A., . . . Group, G. P. A. (2011). The variant call format and VCFtools. *Bioinformatics, 27*(15), 2156-2158. doi:10.1093/bioinformatics/btr330

Davey, J. W., Hohenlohe, P. A., Etter, P. D., Boone, J. Q., Catchen, J. M., & Blaxter, M. L. (2011). Genome-wide genetic marker discovery and genotyping using next-generation sequencing. *Nature Reviews Genetics, 12*(7), 499-510. doi:10.1038/nrg3012

Embke, H. S., Rypel, A. L., Carpenter, S. R., Sass, G. G., Ogle, D., Cichosz, T., . . . Vander Zanden, M. J. (2019). Production dynamics reveal hidden overharvest of inland recreational fisheries. *Proceedings of the National Academy of Sciences, 116*(49), 24676. doi:10.1073/pnas.1913196116

Garza, J. C., & Freimer, N. B. (1996). Homoplasy for size at microsatellite loci in humans and chimpanzees. *Genome Research, 6*(3), 211-217. doi:10.1101/gr.6.3.211

Hammen, J. J., & Sloss, B. L. (2019). Walleye Genetic Characterization in the Northern Ceded Territory of Wisconsin: Implications for Stocking Using Conservation Strategies. *North American Journal of Fisheries Management, 0*(0). doi:10.1002/nafm.10302

Hansen, J., Sass, G., Gaeta, J., Hansen, G., Isermann, D., Lyons, J., . . . Carpenter, S. (2015). Largemouth Bass Management in Wisconsin: Intra- and Inter-Specific Implications of Abundance Increases.

Hoffman, J. I., Simpson, F., David, P., Rijks, J. M., Kuiken, T., Thorne, M. A. S., . . . Dasmahapatra, K. K. (2014). High-throughput sequencing reveals inbreeding depression in a natural population. *Proceedings of the National Academy of Sciences, 111*(10), 3775. doi:10.1073/pnas.1318945111

Jombart, T., & Ahmed, I. (2011). adegenet 1.3-1: new tools for the analysis of genome-wide SNP data. *Bioinformatics, 27*(21), 3070-3071. doi:10.1093/bioinformatics/btr521

Keenan, K., McGinnity, P., Cross, T. F., Crozier, W. W., & Prodöhl, P. A. (2013). diveRsity: An R package for the estimation and exploration of population genetics parameters and their associated errors. *Methods in Ecology and Evolution, 4*(8), 782-788. doi:10.1111/2041-210X.12067

Larson, W. A., Seeb, J. E., Pascal, C. E., Templin, W. D., Seeb, L. W., & Taylor, E. (2014). Single-nucleotide polymorphisms (SNPs) identified through genotyping-by-sequencing improve genetic stock identification of Chinook salmon ( Oncorhynchus tshawytscha) from western Alaska. *Canadian Journal of Fisheries & Aquatic Sciences, 71*(5), 698-708. doi:10.1139/cjfas-2013-0502

Logsdon, D. E., Anderson, C. S., & Miller, L. M. (2016). Contribution and Performance of Stocked Walleyes in the Recovery of the Red Lakes, Minnesota, Fishery. *North American Journal of Fisheries Management, 36*(4), 828-843. doi:10.1080/02755947.2016.1167143

Luikart, G., & England, P. R. (1999). Statistical analysis of microsatellite DNA data. *Trends in Ecology & Evolution, 14*(7), 253-256. doi:10.1016/S0169-5347(99)01632-8

McKinney, G. J., Pascal, C. E., Templin, W. D., Gilk-Baumer, S. E., Dann, T. H., Seeb, L. W., & Seeb, J. E. (2019). Dense SNP panels resolve closely related Chinook salmon populations. *Canadian Journal of Fisheries and Aquatic Sciences*. doi:10.1139/cjfas-2019-0067

McKinney, G. J., Seeb, J. E., & Seeb, L. W. (2017). Managing mixed-stock fisheries: genotyping multi-SNP haplotypes increases power for genetic stock identification. *Canadian Journal of Fisheries and Aquatic Sciences, 74*(4), 429-434. doi:10.1139/cjfas-2016-0443

McKinney, G. J., Waples, R. K., Pascal, C. E., Seeb, L. W., & Seeb, J. E. (2018). Resolving allele dosage in duplicated loci using genotyping-by-sequencing data: A path forward for population genetic analysis. *Molecular Ecology Resources, 18*(3), 570-579. doi:10.1111/1755-0998.12763

McKinney, G. J., Waples, R. K., Seeb, L. W., & Seeb, J. E. (2017). Paralogs are revealed by proportion of heterozygotes and deviations in read ratios in genotyping-by-sequencing

data from natural populations. *Mol Ecol Resour, 17*(4), 656-669. doi:10.1111/1755-0998.12613

Meek, M. H., & Larson, W. A. (2019). The future is now: Amplicon sequencing and sequence capture usher in the conservation genomics era. *Molecular Ecology Resources, 19*(4), 795-803. doi:10.1111/1755-0998.12998

Moran, B. M., & Anderson, E. C. (2018). Bayesian inference from the conditional genetic stock identification model. *Canadian Journal of Fisheries & Aquatic Sciences, 76*(4), 551-560. doi:10.1139/cjfas-2018-0016

Morin, P. A., Luikart, G., Wayne, R. K., & the, S. N. P. w. g. (2004). SNPs in ecology, evolution and conservation. *Trends in Ecology & Evolution, 19*(4), 208-216. doi:https://doi.org/10.1016/j.tree.2004.01.009

Narum, S. R., Buerkle, C. A., Davey, J. W., Miller, M. R., & Hohenlohe, P. A. (2013). Genotyping-by-sequencing in ecological and conservation genomics. *Mol Ecol, 22*(11), 2841-2847. doi:10.1111/mec.12350

Natesh, M., Taylor, R. W., Truelove, N. K., Hadly, E. A., Palumbi, S. R., Petrov, D. A., & Ramakrishnan, U. (2019). Empowering conservation practice with efficient and economical genotyping from poor quality samples. *Methods in Ecology and Evolution, 10*(6), 853-859. doi:10.1111/2041-210X.13173

Navajas, M. J., Thistlewood, H. M. A., Lagnel, J., & Hughes, C. (1998). Microsatellite sequences are under-represented in two mite genomes. *Insect Molecular Biology, 7*(3), 249-256. doi:10.1111/j.1365-2583.1998.00066.x

Pavinato, V. A. C., Wijeratne, S., Spacht, D., Denlinger, D. L., Meulia, T., & Michel, A. P. (2019). Leveraging targeted sequencing for non-model species: a step-by-step guide to obtain a reduced SNP set and a pipeline to automate data processing in the Antarctic Midge, <em>Belgica antarctica</em&gt. *bioRxiv*, 772384. doi:10.1101/772384

Reid, K., Carlos Garza, J., Gephard, S. R., Caccone, A., Post, D. M., & Palkovacs, E. P. (2019). Restoration-mediated secondary contact leads to introgression of alewife ecotypes separated by a colonial-era dam. *Evolutionary Applications, n/a*(n/a). doi:10.1111/eva.12890

Rochette, N. C., Rivera-Colón, A. G., & Catchen, J. M. (2019). Stacks 2: Analytical methods for paired-end sequencing improve RADseq-based population genomics. *Molecular Ecology, 28*(21), 4737-4754. doi:10.1111/mec.15253

Rychlik, W. (1993). Selection of Primers for Polymerase Chain Reaction. In B. A. White (Ed.), *PCR Protocols: Current Methods and Applications* (pp. 31-40). Totowa, NJ: Humana Press.

Rypel, A. L., Goto, D., Sass, G. G., & Zanden, M. J. V. (2018). Eroding productivity of walleye populations in northern Wisconsin lakes. *Canadian Journal of Fisheries and Aquatic Sciences, 75*, 2291+.

Schmidt, D., Campbell, N. R., Govindarajulu, P., Larsen, K. W., & Russello, M. A. (2019). Genotyping-in-Thousands by sequencing (GT-seq) panel development and application to minimally-invasive DNA samples to support studies in molecular ecology. *Molecular Ecology Resources, 0*(ja). doi:10.1111/1755-0998.13090

Seeb, J. E., Carvalho, G., Hauser, L., Naish, K., Roberts, S., & Seeb, L. W. (2011). Single-nucleotide polymorphism (SNP) discovery and applications of SNP genotyping in nonmodel organisms. *Molecular Ecology Resources, 11*, 1-8. doi:10.1111/j.1755-0998.2010.02979.x

Singh, U. A., Kumari, M., & Iyengar, S. (2018). Method for improving the quality of genomic DNA obtained from minute quantities of tissue and blood samples using Chelex 100 resin. *Biological Procedures Online, 20*.

Smith, C. T., Antonovich, A., Templin, W. D., Elfstrom, C. M., Narum, S. R., & Seeb, L. W. (2007). Impacts of Marker Class Bias Relative to Locus-Specific Variability on Population Inferences in Chinook Salmon: A Comparison of Single-Nucleotide Polymorphisms with Short Tandem Repeats and Allozymes. *Transactions of the American Fisheries Society, 136*(6), 1674-1687. doi:10.1577/T06-227.1

Stepien, C., A., Murphy, D., J., Lohner, R., N., Sepulveda-Villet O, J., & Haponski, A., E. (2009). Signatures of vicariance, postglacial dispersal and spawning philopatry: population genetics of the walleye Sander vitreus. *Molecular Ecology, 18*(16), 3411-3428. doi:10.1111/j.1365-294X.2009.04291.x

Storer, C. G., Pascal, C. E., Roberts, S. B., Templin, W. D., Seeb, L. W., & Seeb, J. E. (2012). Rank and Order: Evaluating the Performance of SNPs for Individual Assignment in a Non-Model Organism. *PLOS ONE, 7*(11), 1-13. doi:10.1371/journal.pone.0049018

Wagner, C. E., Keller, I., Wittwer, S., Selz, O. M., Mwaiko, S., Greuter, L., . . . Seehausen, O. (2013). Genome-wide RAD sequence data provide unprecedented resolution of species boundaries and relationships in the Lake Victoria cichlid adaptive radiation. *Molecular Ecology, 22*(3), 787-798. doi:10.1111/mec.12023

Westbrook, L. J. (2012). *Genetic structure of rock bass and johnny darters: Implications for gamefish management in Wisconsin.* (Master's), University of Wisconsin, Stevens Point,

Willi, Y., van Kleunen, M., Dietrich, S., & Fischer, M. (2007). Genetic rescue persists beyond first-generation outbreeding in small populations of a rare plant. *Proceedings of the Royal Society B: Biological Sciences, 274*(1623), 2357-2364. doi:10.1098/rspb.2007.0768

## Data accessibility

Raw data for the RADseq and GT-seq data obtained in this study was deposited to the NCBI sequence read archive (SUB####) and VCF files of genotypes are available on DRYAD (DOI: PENDING). Python and R scripts used in the statistical analysis pipeline are available at GIT

## Author contributions

WL, GS, KG, and LM designed the study with input from MB. Data analyses were conducted by MB with assistance from GM. Laboratory analysis was conducted by MB, KG, and LS. All authors contributed to the writing of the manuscript.

## Tables

**Table 1.** Information on walleye *Sander vitreus* collections from 23 sites in Wisconsin and Minnesota. Reporting units are aggregations of genetically similar populations grouped for GSI analysis, n past filters is the number of individuals missing genotypes at < 30% of SNPs and retained after quality filtering. Diversity statistics calculated using 20,579 SNPs. The $F_{ST_600}$, $Composite_{_600}$, and $Diversity_{_600}$ columns are the percent correct assignment to reporting group for each population with 100% simulations conducted using the corresponding panel.

| Population ID | Reporting Unit | Population | Latitude | Longitude | n sampled | n past filters | $H_E$ | $H_O$ | $F_{IS}$ | AR | $F_{ST_600}$ | $Composite_{_600}$ | $Diversity_{_600}$ |
|---|---|---|---|---|---|---|---|---|---|---|---|---|---|
| 1 | Rock-Fox | Delavan Lake | 42.58 | -88.63 | 48 | 48 | 0.169 | 0.168 | 0.008 | 1.607 | 1.00 | 1.00 | 1.00 |
| 2 | Wolf River | Lake Winnebago | 44.36 | -88.69 | 47 | 41 | 0.173 | 0.186 | -0.05 | 1.645 | 1.00 | 1.00 | 1.00 |
| 3 | Upper Wisconsin | Lake Wisconsin | 43.38 | -89.58 | 48 | 45 | 0.179 | 0.175 | 0.017 | 1.674 | 1.00 | 1.00 | 1.00 |
| 4 | Upper Wisconsin | Medicine Lake Chain | 45.81 | -89.13 | 47 | 47 | 0.166 | 0.166 | 0.004 | 1.604 | 0.96 | 0.98 | 0.98 |
| 5 | Upper Wisconsin | Willow Flowage | 45.71 | -89.87 | 48 | 48 | 0.176 | 0.174 | 0.013 | 1.657 | 1.00 | 1.00 | 0.99 |
| 6 | Upper Wisconsin | Kawaguesaga Lake | 45.86 | -89.74 | 48 | 42 | 0.17 | 0.167 | 0.013 | 1.638 | 0.96 | 0.94 | 0.94 |
| 7 | Upper Wisconsin | Big Arbor Vitae Lake | 45.93 | -89.65 | 48 | 44 | 0.174 | 0.174 | 0.005 | 1.654 | 0.74 | 0.96 | 0.99 |
| 8 | Upper Chippewa | Escanaba Lake | 46.06 | -89.59 | 48 | 44 | 0.168 | 0.173 | -0.018 | 1.623 | NA | NA | NA |
| 9 | Upper Chippewa | Sanford Lake | 46.18 | -89.69 | 48 | 44 | 0.157 | 0.164 | -0.033 | 1.528 | NA | NA | NA |
| 10 | Upper Chippewa | Manitowish Lake | 46.11 | -89.85 | 47 | 35 | 0.172 | 0.175 | -0.006 | 1.647 | 0.58 | 0.57 | 0.51 |
| 11 | Upper Chippewa | Turtle Flambeau Flowage | 46.06 | -90.13 | 47 | 38 | 0.173 | 0.172 | 0.005 | 1.661 | 0.63 | 0.55 | 0.76 |
| 12 | Upper Chippewa | Chippewa Flowage | 45.90 | -91.09 | 47 | 43 | 0.173 | 0.175 | -0.006 | 1.658 | 0.88 | 0.89 | 0.93 |
| 13 | Upper Chippewa | Eau Claire River | 44.80 | -91.50 | 47 | 47 | 0.161 | 0.162 | -0.001 | 1.583 | 0.98 | 0.98 | 0.98 |
| 14 | Upper Chippewa | Lake Millicent | 46.53 | -91.37 | 48 | 32 | 0.167 | 0.176 | -0.034 | 1.623 | NA | NA | NA |
| 15 | Lake Superior | St. Louis River | 46.65 | -92.21 | 32 | 30 | 0.17 | 0.168 | 0.006 | 1.621 | 0.77 | 0.77 | 0.77 |
| 16 | Vermilion River | Pike River | 47.59 | -92.39 | 32 | 28 | 0.144 | 0.142 | 0.005 | 1.498 | 1.00 | 1.00 | 1.00 |
| 17 | Des Moines River | Lake Sarah | 44.15 | -95.77 | 32 | 30 | 0.164 | 0.166 | -0.006 | 1.597 | 1.00 | 1.00 | 1.00 |
| 18 | North Fork Crow River | Lake Koronis | 45.33 | -94.70 | 32 | 17 | 0.155 | 0.155 | -0.011 | 1.579 | 0.82 | 0.82 | 0.75 |
| 19 | Rum River | Mille Lacs Lake | 46.25 | -93.67 | 32 | 29 | 0.148 | 0.151 | -0.018 | 1.511 | 1.00 | 1.00 | 1.00 |
| 20 | Pine River | Pine River | 46.70 | -94.39 | 32 | 30 | 0.156 | 0.162 | -0.028 | 1.547 | 0.97 | 0.97 | 0.97 |
| 21 | Mississippi River - Headwaters | Cutfoot Sioux Lake | 47.50 | -94.09 | 32 | 25 | 0.147 | 0.148 | -0.011 | 1.517 | 1.00 | 1.00 | 1.00 |
| 22 | Otter Tail River | Ottertail Lake | 46.41 | -95.66 | 32 | 23 | 0.158 | 0.16 | -0.016 | 1.568 | 1.00 | 1.00 | 0.97 |
| 23 | Red Lake | Red Lake | 47.91 | -95.04 | 32 | 29 | 0.149 | 0.153 | -0.025 | 1.514 | 0.90 | 0.86 | 0.83 |

**Table 2.** Summary of pairwise $F_{ST}$ comparisons between walleye *Sander vitreus* populations grouped by state of origin. Abbreviations are Wisconsin (WI) and Minnesota (MN).

| | **WI-WI** | **MN-MN** | **WI-MN** |
|---|---|---|---|
| Max | 0.106 | 0.142 | 0.142 |
| Mean | 0.032 | 0.068 | 0.072 |
| Min | 0.001 | 0.019 | 0.026 |

898 **Table 3.** Summary statistics by SNP panel tested for walleye *Sander vitreus* in Wisconsin and
899 Minnesota, USA, including: average $F_{ST}$, heterozygosity ($H_{E_mhap}$), assignment accuracy to
900 population and reporting unit of origin in 100% simulations, and estimated false-positive rates
901 (FPR) for a given kin relationship at a false-negative rate (FNR) of 0.01.

902

| | $F_{ST_600}$ | Composite$_{_600}$ | Diversity$_{_600}$ |
|---|---|---|---|
| Average $F_{ST}$ | 0.117 | 0.076 | 0.047 |
| Average $H_{E_mhap}$ | 0.389 | 0.569 | 0.633 |
| Average accuracy by reporting unit | 0.937 | 0.937 | 0.929 |
| Average accuracy by population | 0.864 | 0.861 | 0.862 |
| Parent-offspring FPR (FNR = 0.01) | $4.68\times10^{-34}$ | $7.92\times10^{-62}$ | $2.74\times10^{-80}$ |
| Full-sibling FPR (FNR = 0.01) | $3.42\times10^{-29}$ | $5.34\times10^{-50}$ | $1.16\times10^{-64}$ |
| Half-sibling FPR (FNR = 0.01) | $6.44\times10^{-6}$ | $2.56\times10^{-10}$ | $2.06\times10^{-13}$ |

903

904

905 **Table 4.** Summary of GT-seq optimization runs for walleye *Sander vitreus* in Wisconsin and
906 Minnesota, USA. Rows report number of primer pairs targeted, number of reads with intact i-7
907 barcodes (retained reads), number of retained reads with *in-silico* primer sequences (total reads),
908 number of total reads with *in-silico* probe sequences (on-target reads), percent of total reads on-
909 target, percent of total reads allocated to the 10% of loci tested with highest rank total read
910 counts, average number of SNPs per locus, and average GC content in the forward and reverse
911 primers.

| | **Test 1** | **Test 2** | **Test 3** |
|---|---|---|---|
| Total primer pairs | 600 | 477 | 436 |
| i7 reads | 4,655,071 | 12,653,262 | 7,282,101 |
| i7 reads w/ primers (total reads) | 4,150,910 | 9,347,591 | 6,827,424 |
| i7 reads w/ primers & probes (on- target) | 1,031,707 | 3,268,293 | 6,262,523 |
| On-target percent of total reads | 24.9% | 35.0% | 91.7% |
| Percent reads in top 10% of loci | 85.0% | 72.5% | 36.6% |
| mean SNPs per locus | 2.06 | 2.00 | 1.97 |
| mean GC percent forward primer | 51.0% | 50.4% | 50.3% |
| mean GC percent reverse primer | 49.0% | 48.3% | 48.2% |
| mean $F_{ST}$ | 0.133 | 0.133 | 0.133 |
| mean $H_{E_mhap}$ | 0.425 | 0.415 | 0.416 |

912

913

914 **Figures**

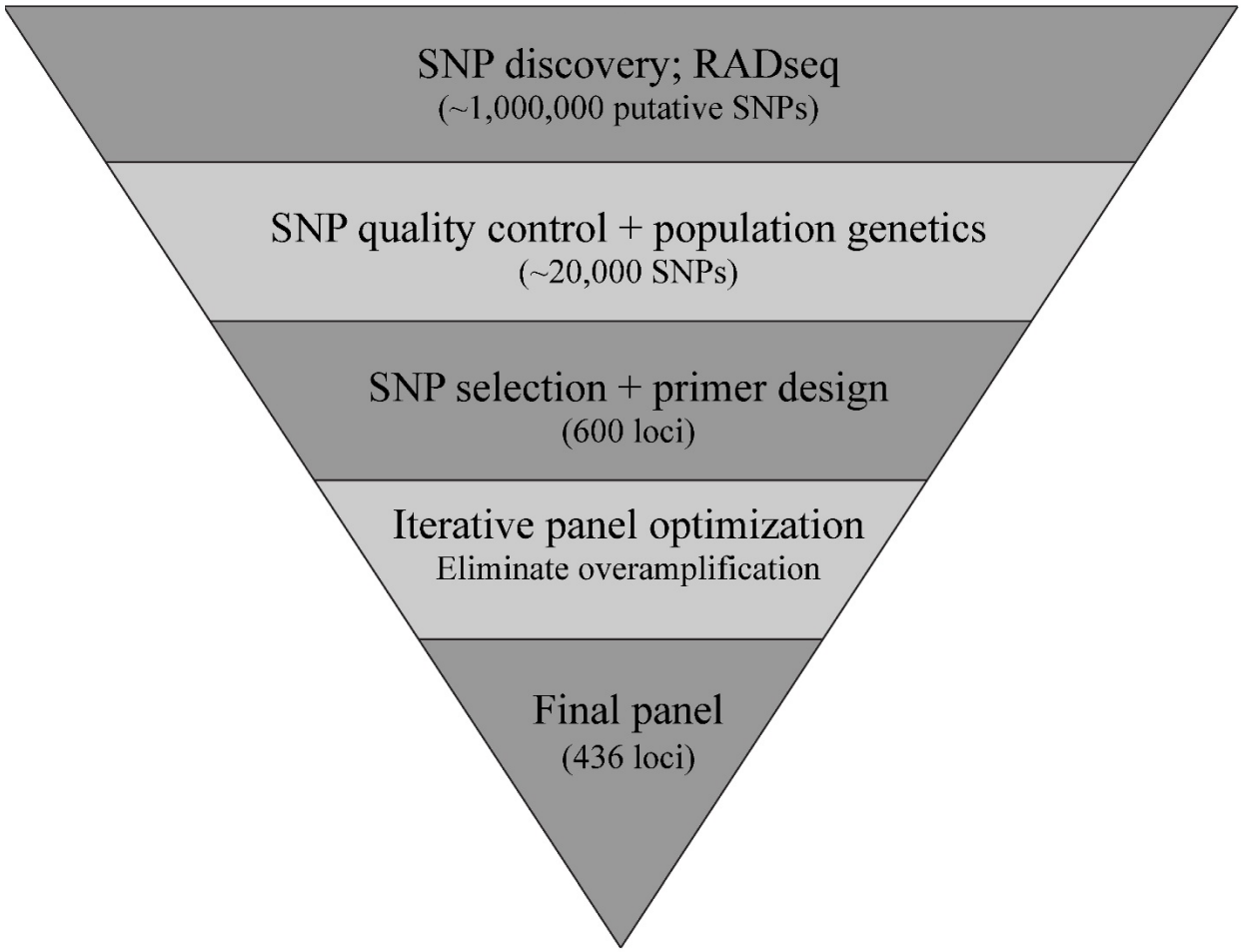


915

916 **Figure 1.** Generalized workflow describing major steps inherent to *de novo* construction of a
917 high-density SNP panel for walleye *Sander vitreus* in Wisconsin and Minnesota, USA. Numbers
918 of SNPs or loci present in each phase for this panel shown in parentheses.

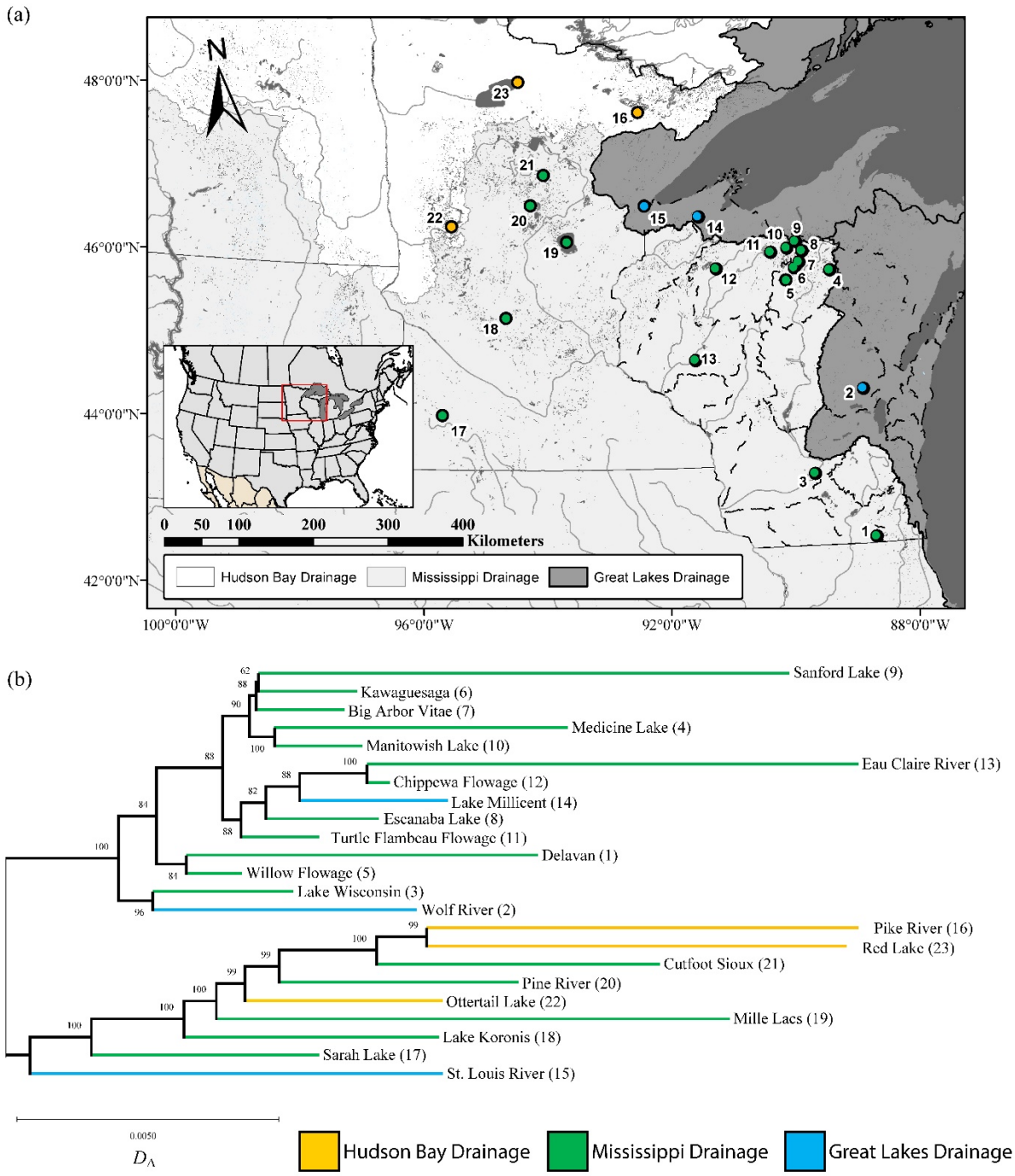


**Figure 2.** (a) Map of walleye *Sander vitreus* in Wisconsin (populations 1-14), the St. Louis River (population 15), and Minnesota (populations 16-23), USA, collection locations and (b) dendrogram of sampled populations with bootstrap support (n = 1000) estimates above nodes. Branch lengths correspond to genetic distances estimated using Nei's $D_A$. Figures color coded according to major drainage of origin (Hudson Bay: yellow, Mississippi: green, Great Lakes: blue) and numbered with respect to order in Table 1.

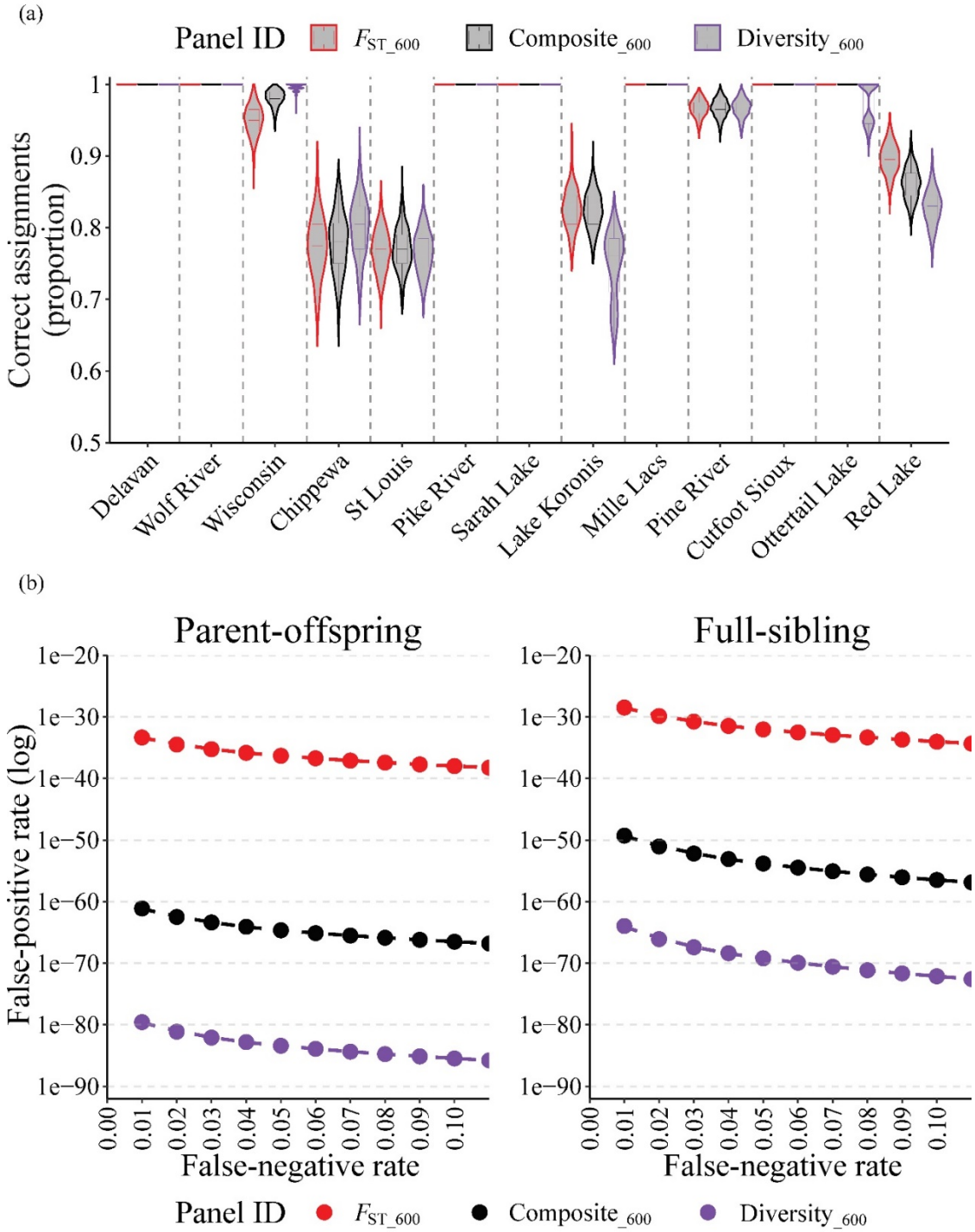


**Figure 3.** (a) Violin plots showing densitity distributions of accuracy estimates from 100% simulations of 23 populations of walleye *Sander vitreus* in Wisconsin and Minnesota, USA, performed using 1,000 iterations for each test panel by reporting unit and (b) simulated false-positive rate (FPR) estimates across a range of false-negative rates (FNR). Figures color coded according to SNP panel tested: $F_{ST_600}$ (red, 600 rank $F_{ST}$ loci), Composite$_{_600}$ (black, 300 rank $F_{ST}$ and 300 rank $H_{E_mhap}$ loci), and Diversity$_{_600}$ (purple, 600 rank $H_{E_mhap}$ loci).

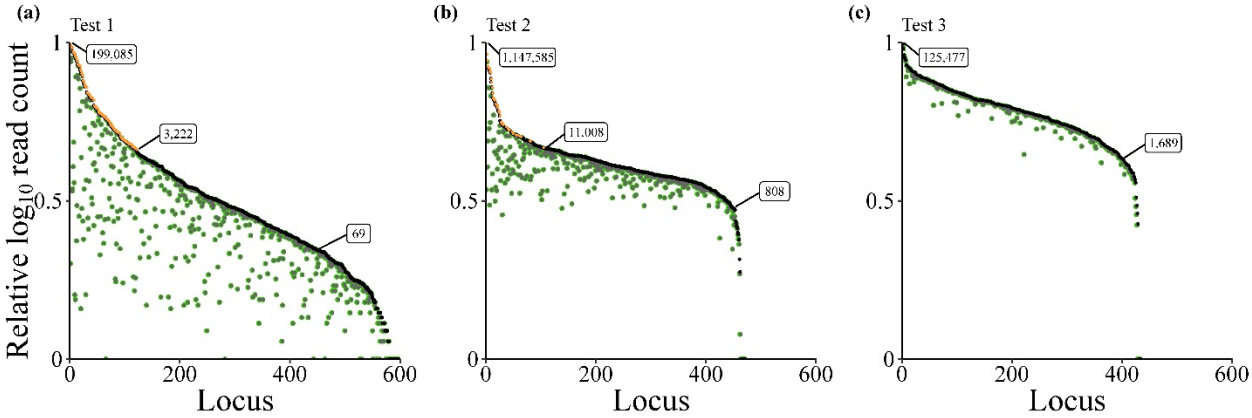


**Figure 4.** Relative $\log_{10}$ total read counts per locus (black) and relative $\log_{10}$ on-target read counts per locus (green) of the GT-seq panel for walleye *Sander vitreus* in Wisconsin and Minnesota, USA, prior to optimization (a, 600 loci), after first optimization (b, 477 loci), and after second optimization (c, 436 loci). Loci identified for culling during optimization steps shown in orange. Raw read counts annotated in boxes.

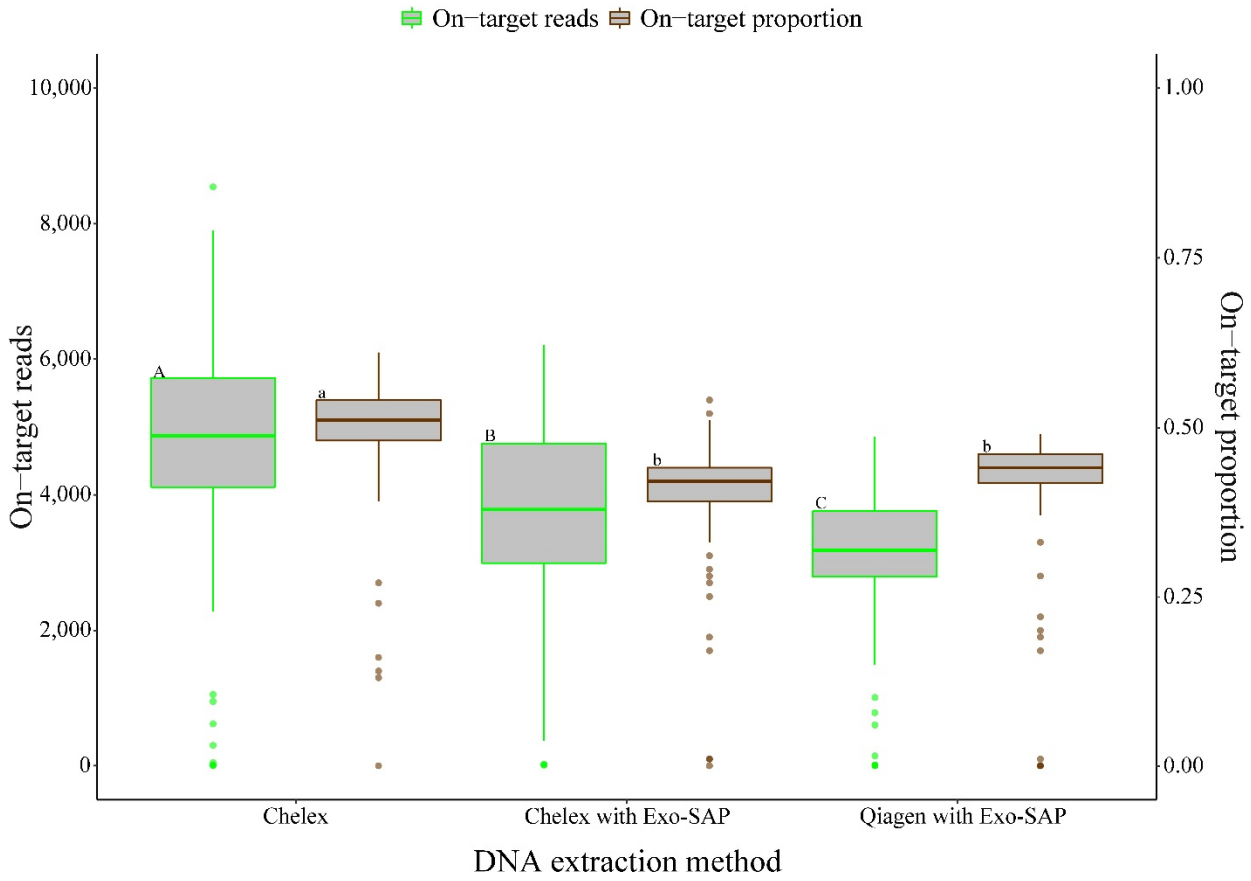


**Figure 5.** Number of on-target reads (green) and proportion of total reads on-target obtained from GT-seq libraries produced using DNAs extracted via Chelex, Chelex with Exo-SAP, and Qiagen with Exo-SAP. Significantly different groups denoted by letters on box.

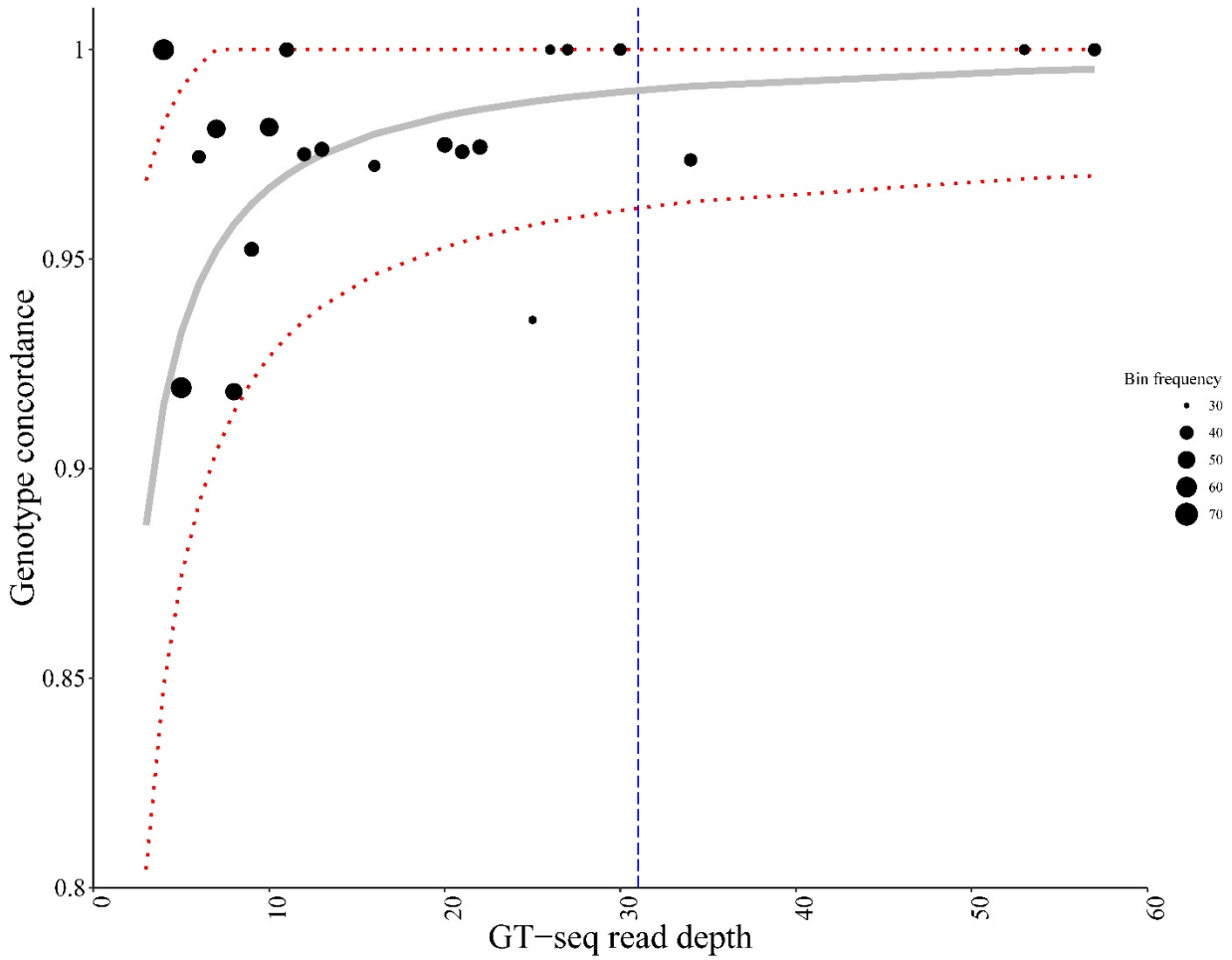


**Figure 6.** Modeled relationship between GT-seq read depth and genotype concordance between GT-seq and RADseq shown in gray (1.00-0.34/GT-seq read depth, rss = 0.02) with 95% confidence intervals in red. GT-seq read depth at which estimated genotype concordance equals 99% (96.2%-100%) represented by blue line. Black points display proportion of genotypes found identical between GT-seq and RADseq for GT-seq read depth bins with > 30 genotypes.

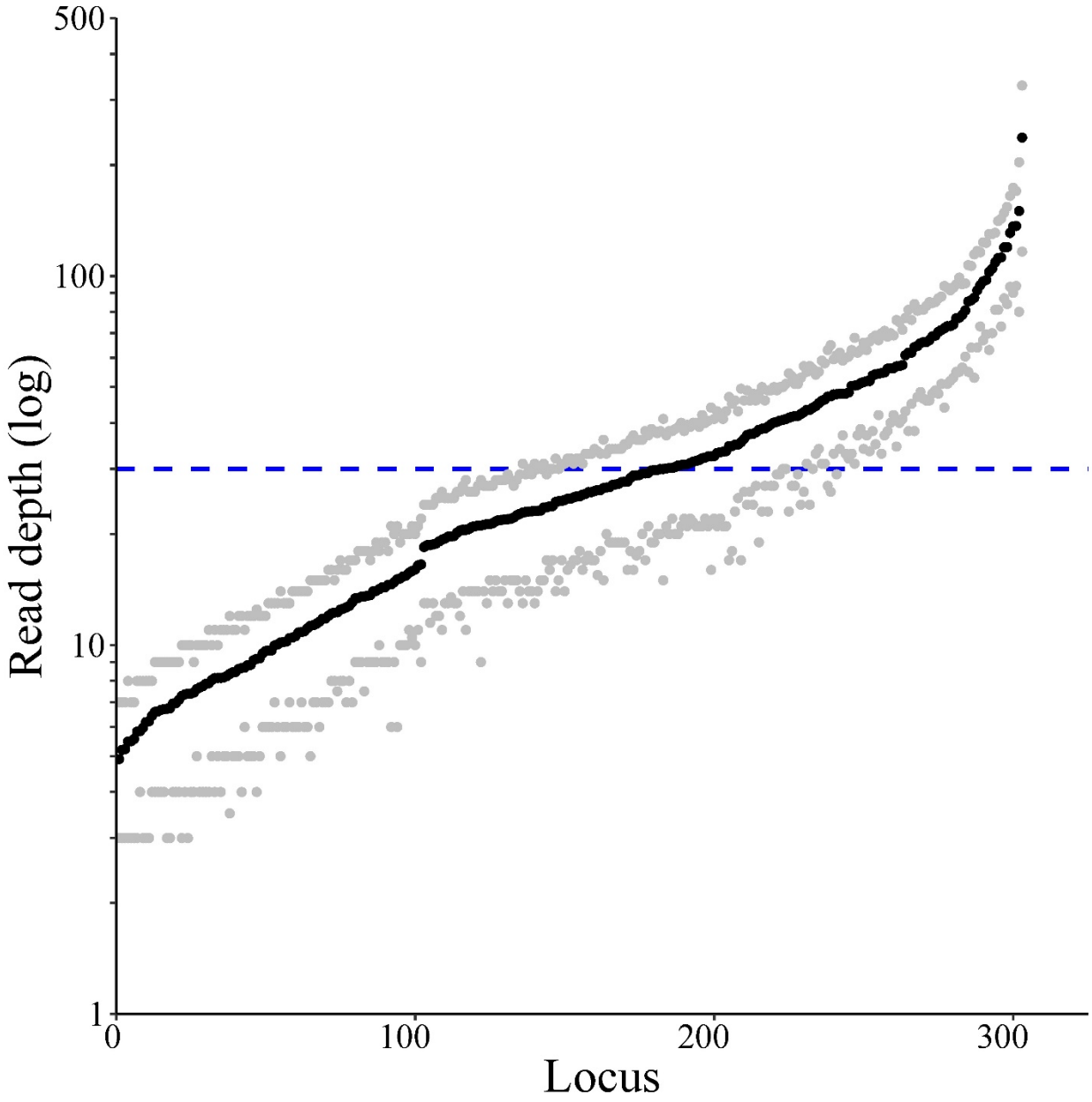


**Figure 7.** Variation in read depth among individuals at loci successfully genotyped after quality filtering (303 loci with < 30% missing data). Average read depth at each locus shown with black points, while gray points denote first and third quartile for each locus. Dotted blue line denotes target read depth of 30×. Data from 551 walleye sequenced using fully optimized panel. Average read depth among all loci is 33×.

957

958 **Supplementary materials**

959 **Table S1.** Pairwise $F_{ST}$ estimates for all sampled walleye *Sander vitreus* populations (sites
960 numbered according to Table 1 and Fig. 1 A). Estimates produced in arlequin v3.5.2.

961 **Table S2.** Summary statistics for 20,597 SNPs retained through initial filtering based on
962 maximum missingness rates of < 30% and HDplot cutoffs of H > 0.5 and -7 < D < 7. Columns
963 include a locus tag (CHROM), position of SNP within locus (Reid et al.), a unique SNP value
964 (ID), reference (REF) and alternate (Keenan et al.) SNP alleles, global $F_{IS}$ (Willi et al.), single
965 SNP $F_{ST}$ (Smith et al.), expected microhaplotype heterozygosity (mhap_$H_E$), and number of
966 alleles per locus tag (n_alleles). Diversity statistics estimated in diveRsity v1.9.90 (global $F_{IS}$ and
967 single SNP $F_{ST}$) and adegenet v2.1.1 (single locus $H_E$, number of alleles).

968 **Table S3.** Summary matrix of 100% simulations (reps = 1,000, mixsize = 200) for each sampled
969 population retained through filtering, performed using the $F_{ST_600}$ panel. Each row represents a
970 simulation for the listed population name. Each column within a row represents the proportion of
971 individuals assigned to the population denoted at the top of the column. Unassigned individuals
972 (< 70% probability of origin from a given population) accounted for in last column.

973 **Table S4.** Summary matrix of 100% simulations (reps = 1,000, mixsize = 200) for each sampled
974 population retained through filtering steps, performed using the Composite$_{_600}$ panel. Each row
975 represents a simulation for the listed population name. Each column within a row represents the
976 proportion of individuals assigned to the population denoted at the top of the column.
977 Unassigned individuals (< 70% probability of origin from a given population) are accounted for
978 in the last column.

979 **Table S5.** Summary matrix of 100% simulations (reps = 1,000, mixsize = 200) for each sampled
980 population retained through filtering steps, performed using the Diversity$_{_600}$ panel. Each row
981 represents a simulation for the listed population name. Each column within a row represents the
982 proportion of individuals assigned to the population denoted at the top of the column.
983 Unassigned individuals (< 70% probability of origin from a given population) are accounted for
984 in the last column.

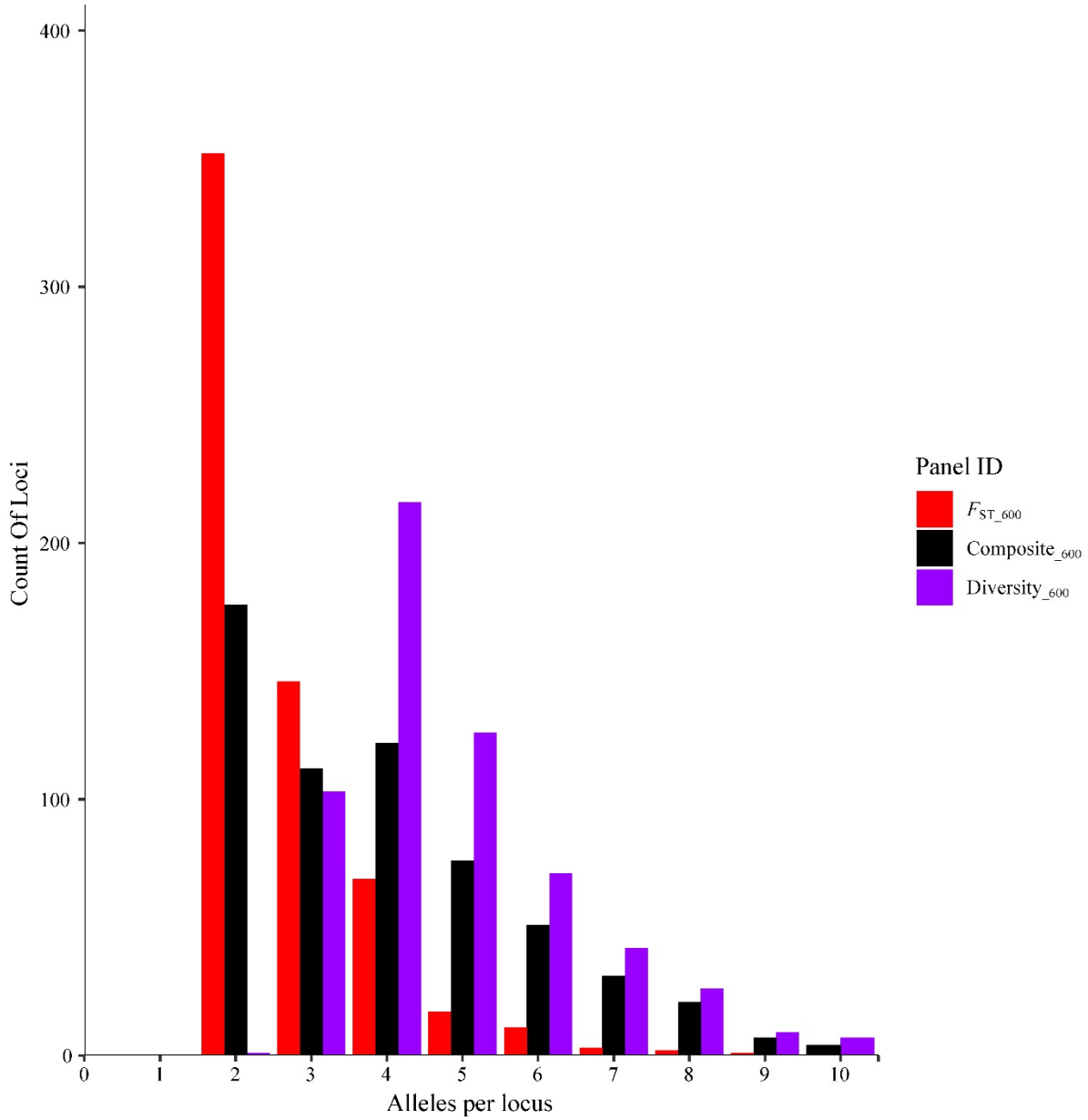


985

986 **Figure S1.** Frequency distribution of number of alleles among 600 loci tested in each panel.